



**PROBABILISTIC ESTIMATION OF RARE RANDOM COLLISIONS
IN 3 SPACE**

THESIS

Timothy Holzmann, Captain, USAF

AFIT/GOR/ENS/09-07

**DEPARTMENT OF THE AIR FORCE
AIR UNIVERSITY
AIR FORCE INSTITUTE OF TECHNOLOGY**

Wright-Patterson Air Force Base, Ohio

APPROVED FOR PUBLIC RELEASE; DISTRIBUTION UNLIMITED.

AFIT/GOR/ENS/09-07

**PROBABILISTIC ESTIMATION OF RARE RANDOM COLLISIONS
IN 3 SPACE**

THESIS
Timothy Holzmann
Captain, USAF

AFIT/GOR/ENS/09-07

APPROVED FOR PUBLIC RELEASE; DISTRIBUTION UNLIMITED.

The views expressed in this thesis are those of the author and do not reflect the official policy or position of the United States Air Force, Department of Defense or the United States Government.

AFIT/GOR/ENS/09-07

**PROBABILISTIC ESTIMATION OF RARE RANDOM
COLLISIONS IN 3 SPACE**

THESIS

Presented to the Faculty
Department of Operational Sciences
Graduate School of Engineering and Management
Air Force Institute of Technology
Air University
Air Education and Training Command
in Partial Fulfillment of the Requirements for the
Degree of Master of Science in Operations Research

Timothy Holzmann, B.A.
Captain, USAF

March 2009

APPROVED FOR PUBLIC RELEASE; DISTRIBUTION UNLIMITED.

**PROBABILISTIC ESTIMATION OF RARE RANDOM
COLLISIONS IN 3 SPACE**

Timothy Holzmann, B.A.

Captain, USAF

Approved:

Jeffery Cochran, Ph.D.
Chairman

Date

Maj Shane Hall, Ph.D.
Member

Date

Joseph Kebir, Ph.D.
Member

Date

Abstract

A study of risk assessment for artillery fire randomly colliding with fixed wing aircraft is presented. The research lends itself to a general study of collision models. Current models of object collisions fall under one of three categories: the historical model, the gas particle model, and the satellite model. These three vary in data requirements and mathematical representation of the impact event. The gas particle model is selected for its flexibility and robust estimation. However, current mathematical development in the literature does not include certain spatial and dynamic components necessary for a general encounter (collision) model. These are derived in this work. For the specific application at hand Quadratic formulas estimate the ballistic arc of artillery shells to provide instantaneous relative velocities. An extended Poisson spatial process is applied over the relative volume within a collision radius during the conflict time window to provide a probability of collision. Implementation of the model for military use has been achieved via an Excel spreadsheet providing scenario study capability in real time. Results for several scenarios are presented which have been validated by experts. These results support current policy of strict deconfliction.

Dedication

This thesis is dedicated to my wife. Her selfless attitude in assuming so many aspects of managing our home, her faithful loving encouragement, and her unyielding belief in my ability to excel, were all crucial to my being able to complete this intense program. As much as this thesis and degree are a testament to my academic abilities, they are even more a testament to her devotion and love. Thank you, darling.

Acknowledgements

I would like to thank my advisor, Dr. Jeffery Cochran, for his great patience and guidance in developing this thesis. His mentorship and encouragement throughout the process have been treasures that I will carry with me in my future career. The members of my thesis committee, Dr. Youcef Kebir and Maj Shane Hall provided excellent feedback and recommendations for improvements.

My thanks also goes to my sponsor, Col J. Roscoe “Rudder” Smith, and his team from AFDDEC/WA. Their continued support and feedback have greatly enhanced the quality of the work presented here. Also, Maj. Glen Shilland, USAF, from AFIT and Maj. Mike Hughes, USA, from the Army TRADOC provided invaluable expertise to develop the case studies. Finally, my thanks also goes to HQ AF/A9 for the verification and validation of the model and their suggestions for improvements.

Timothy Holzmann

Table of Contents

	Page
Abstract	iv
Acknowledgements	vi
List of Figures	x
List of Tables	xi
List of Symbols	xii
1. Introduction	1-1
1.1 Setting	1-1
1.2 Problem Statement	1-2
1.2.1 Background on Encounter models	1-2
1.2.2 Discussion	1-7
1.3 Objective	1-8
1.4 Scope	1-8
1.5 Overview	1-11
2. Theoretical Development	2-1
2.1 Introduction	2-1
2.1.1 The Difficulty on Dynamic SPPs	2-1
2.1.2 The Extended Poisson Process	2-3
2.1.3 Outline	2-4
2.2 Definitions, Assumptions, and Scenario Description	2-5
2.2.1 Defining locations and motion	2-5
2.2.2 Defining an encounter region	2-8

	Page	
2.3	\vec{v} as a function of S	2-13
2.4	The Extended Spatial Poisson Process	2-16
2.5	Conclusion	2-21
3.	Case Study	3-1
3.1	Introduction and Problem Description	3-1
3.2	Finding the Right Model	3-2
3.3	Model Development	3-4
3.3.1	<i>Step 1: Relative Velocity (Applying Ballistic Formulas)</i>	3-5
3.3.2	<i>Step 2: Shell Density (Applying Spatial Point Process Theory)</i>	3-8
3.3.3	<i>Step 3: Probabilistic Estimation (Applying Numerical Integration)</i>	3-10
3.4	Sensitivity Analysis	3-12
3.5	Numerical Results	3-15
3.5.1	Scenario 1	3-17
3.5.2	Scenario 2	3-17
3.5.3	Scenario 3	3-18
3.5.4	Further discussion	3-19
3.6	Conclusion	3-20
4.	Conclusion	4-1
4.1	Research Summary	4-1
4.2	Future Work	4-1
Appendix A.	Blue Dart	A-1
Appendix B.	Poster Chart	B-1

	Page
Appendix C. Excel Model User Guide	C-1
C.1 Worksheet 1: “Start Here”	C-1
C.1.1 The Model Calculator	C-1
C.1.2 The Unit Converter	C-4
C.1.3 The Data Suggestions	C-4
C.1.4 Graphs	C-6
C.2 Inputs & Outputs	C-6
C.3 GaussQuad	C-6
Bibliography	BIB-1

List of Figures

Figure		Page
1.1.	The Problem Scenario	1-9
2.1.	The leading edge in 2 dimensions	2-10
3.1.	The Problem Scenario	3-2
3.2.	Model flow chart.	3-5
3.3.	The geometry of relative velocities.	3-6
3.4.	Computing the probability of angle of incidence.	3-6
3.5.	Software implementation screenshot.	3-14
3.6.	p by v_m and y	3-15
3.7.	p by v_m and v_a	3-16
3.8.	p by v_a and r	3-16
3.9.	Comparing the probability of no fratricide to collision radii .	3-18
3.10.	Comparing the probability of no fratricide to scenario duration	3-18
C.1.	A screen shot of the Excel model	C-2
C.2.	Excerpt from FM 6-40 containing standard firing conditions .	C-3
C.3.	The conversion table	C-5
C.4.	Table of Baseline Data	C-5
C.5.	Screenshot of “GaussQuad” worksheet	C-8

List of Tables

Table		Page
2.1.	Velocity inputs for example problem	2-19
2.2.	Scenario inputs for example problem	2-19
C.1.	Clarification on column meanings for “GaussQuad” worksheet	C-7

List of Symbols

Symbol	Page
Spatial point process: SPP	2-1
Set of locally finite point configurations: N_{lf}	2-1
Relative speed: v_{rel}	2-2
Lebesgue measure: μ	2-5
Speed: \mathbf{v}	2-6
“distributed as”: \sim	2-7
Path: p	2-8
Jacobian: $J_p(p(t))$	2-8
Closed ball: $\beta_{(d,r)}(s)$	2-8
Encounter window: $W_r(p, \Delta t)$	2-9
Leading edge: $LE_p(s)$	2-9
Incremental encounter window: $W_r^*(p, \delta t)$	2-11
Lebesgue measure adjusted for relative motion: $\mu_{(d,rel)}^{(\vec{v}_A, \vec{v}_B)}$	2-14
Probability of n arrivals: \mathbf{p}_n	2-17
Speed of object a : v_a	3-5
Shell speed: v_s	3-5
Angle of incidence: ϑ	3-5
Artillery angle of elevation: θ	3-7
Muzzle velocity: v_m	3-7
Gravitational constant: g	3-7
Vertical component of muzzle velocity: v_v	3-9
Max ord: h	3-9
Queue type: M/D/ ∞	3-9
Number of shells in the aircraft altitude window: L	3-9
Total encounter airspace volume: W_T	3-10

Symbol	Page
Shell density: σ_X	3-10
Coefficient for Gaussian Quadrature: $c_x(t_x)$	3-12

PROBABILISTIC ESTIMATION OF RARE RANDOM COLLISIONS IN 3 SPACE

1. Introduction

1.1 Setting

The date was March 21, 2001. The spring training game between the Arizona Diamondbacks and the New York Giants was in its 7th inning. Randy Johnson wound up to pitch his famous hardball, released, . . . and . . . the ball was HIT . . . by a bird! (Campbell, 2001)

Random collisions occur all around us every day. Meteor strikes, particles of air colliding, midair aircraft collisions, and subatomic particles smashing together in nuclear reactors are a few examples. Some collisions seem mundane, and others seem like an amazing coincidence. Some are completely uninteresting, but others grab our attention with the enormity of the event. Generalizing on the concept of collisions, there are many interactions requiring that objects pass within some distance of the center of each other to stimulate some event. Such events are called “encounters” – where one object encounters the other in space. Search and rescue operations require that the searchers pass within some detection distance in order to find the victims. Wireless networks require that the client is within a certain distance of the hub in order to maintain the required signal strength.

If the motion of the two objects can be represented by some random variable, then their encounter is a random event and can be probabilistically estimated. Such probabilistic estimates have repeatedly been requested regarding various encounter scenarios throughout history. It is argued that the first question regarding random

encounters was in the desire to avoid rainfall by running. However, that particular scenario was not posed in the literature until the late 20th century.

The earliest probability estimate of an encounter model dates back to the work of Rudolph Clausius in the mid-nineteenth century. Clausius was advocating a kinetic theory of heat. At the time, it was thought that heat was some type of substance, called *caloric* that was transferred from one object to another. Clausius believed, as is commonly held in the scientific community today, that heat was rather the kinetic energy of the molecules making up the object. One primary objection to Clausius' theory was the issue of dissipating vapors: if the gas particles really moved as fast as Clausius claimed, why did it take so long for smoke to dissipate from one side of the room to the other. Clausius' response was to point out that the motions of particles are not "free," rather they are inhibited by collisions with other particles randomly dispersed throughout the space. He proceeded to demonstrate that the amount of distance a particle can travel before it randomly collides with another particle is sufficient to prevent instantaneous dispersal of a vapor (Brush, 1965).

1.2 Problem Statement

Understanding the issues regarding encounter models requires one to first appreciate the different types of models there are and the variety of real-world encounter scenarios they represent.

1.2.1 Background on Encounter models

Encounter models fall into one of three categories discussed below.

1.2.1.1 The Historical Model

The historical model derives its name from the general concept of taking historical data where similar incident objects have moved in a space populated by similar target objects and considers the ratio of collision incidences to collision-free inci-

dences for an estimate of the probability of future collisions. The model is widely used in many different topical studies. Mathematically, it is very simple and extremely useful in cases where it is impossible or undesirable to characterize the motion paths of the objects whether by stochastic or deterministic means. This model has been used to estimate collision probabilities in a variety of scenarios including bird strikes on aircraft (Bird/Wildlife Avian Strike Hazard (BASH) Team, 2008), meteor collisions on earth (Chapman and Morrison, 1994), and the general concept was also used in studies on Tomahawk cruise missile fratricides (Pollack et al., 1997) and satellite collisions (Carpenter, 2007).

In each of the above cases it would have been extremely difficult to model the motion paths of the incident object, the target objects, or both. For example, in the case of bird strikes it would be reasonable to expect the birds and the pilots to exhibit avoidance behavior when they sense a collision is impending. On the other hand, it is much simpler to simply examine cases where collisions occurred and where they did not occur, and take the ration of collision scenarios to all scenarios as the probability of collision.

The historical model's primary benefits are its simplicity and flexibility. It requires an input of the number of collision events and the number of non-collision events. The probability of collision is then estimated by

$$p_c = \frac{\# \text{ collisions}}{[\# \text{ collisions}] + [\# \text{ non-collisions}]}$$

Alternatively, in the case of continuous time parameters, it would also suffice to have several samples of disjoint time intervals t_i for $i = 1, 2, \dots, n$, each with a corresponding count of the collisions that occurred during that interval, $N(t_i)$. Then an estimate for the number of events in some future time interval, t^* , is given by

multiplying the expected collision rate by the specified time interval:

$$p_c = \left(\sum_{i=1}^n \frac{N(t_i)}{nt_i} \right) t^*$$

The flexibility is demonstrated by its ability to deal with avoidance behavior as mentioned previously, and it is demonstrated by the model’s ability to accept even quasi-“historical” data from Monte Carlo simulations such as the ones in the Tomahawk study (Pollack et al., 1997). The simplicity allows for fast computation of collision probabilities where the data is readily available. For example, meteor collision models consider the rate of meteor strikes and multiply this by the prior probability of a meteor being of a certain size. This is used in doomsday calculations for the probability of a meteor destroying the human race within the next 100 years (Chapman and Morrison, 1994).

The largest difficulty with the historical model is the standard question of all sampled data: is the data truly representative of the whole population? One solution for the problem is to strip away the quantitative results and simply give a qualitative or comparative output (i.e., “You are more likely to encounter object *a* than you are encounter with object *b*”). This is the approach taken by the Bird/Wildlife Aircraft Strike Hazard Team in the United States Air Force Avian Hazard Advisory System (Bird/Wildlife Avian Strike Hazard (BASH) Team, 2008). Another answer to the problem of sampling data is by limiting the number of scenarios. The Tomahawk limits the study to only the scenarios that are most likely to result in a fratricide and thus uses the worst-case scenario to provide an upper bound on the probability of collision for an arbitrary scenario (Pollack et al., 1997).

1.2.1.2 The Gas Particle Model

The gas particle model is a very commonly used model for estimating collisions or general encounter probabilities. In this model an incident particle moves through the space at a constant velocity. No information is required or assumptions made

about the location or path of the incident or target particle paths, except that they are uniformly distributed throughout the space. All objects are treated as point particles and collisions occur when the incident particles come within a defined radial distance from the target particles. Using the radial distance and a constant forward velocity, the incident particles "search" through a measurable volume (or area for two dimensional spaces) in a time interval. The target particle density is then computed over the searched area to estimate the expected number of collisions. The rate of collision is the searched area divided by the total area. This rate is converted to a probability by using a Poisson arrival process for the collisions.

The model has been heavily researched and applied to many different scenarios. As the name suggests, this model is used to examine gas particle interactions (Clausius, 1858). Other application domains for the gas particle model include

- Sub-atomic collision models (Johnson, 1939)
- Minefield navigation (Inselmann, 1977; Kim, 2002)
- Orbital debris field calculations (Jenkin and Gick, 2002; Johnson et al., 2001)
- The question: "Will I stay drier by running in the rain?" (DeAngelis, 1987)
- Bird strikes on windmills (Ano, 2000)
- Aircraft collision probabilities under "free flight" rules (Alexander, 1970)

Many simple applications limit themselves to mean value analysis by assuming a constant density, however, no such limitation is required by the literature. Non-constant densities and constant density probabilities are handled by spatial point processes (SPPs). SPPs are used in a wide variety of fields including forestry, geography, seismology, cosmology, spatial epidemiology, and material sciences (see for example: Brix and Chadoeuf (2002); Comas and Mateu (2007)). Several common SPPs are the binomial, Poisson, Cox, and Gibbs processes. They frequently assume stationary points, but not always (Møller and Waagepetersen, 2006). Examples of

non-stationary, or “dynamic,” models include epidemiological models with migration allowed (Ball and Lynn, 2006) and sphere packing models (Stoyan, 2003). More specific to the encounter modeling domain, kinetic theory and orbital debris environment models dynamic point processes of the Poisson variety to generate collision probabilities.

Angelis’ (1987) solution to the rainfall question will mathematically map into the gas particle construct, however his particular solution incorporates the flux of rainfall against a unit surface. This demonstrates a key concept of the model: relative motion. In Angelis’ formulation, he takes the frame of reference of a stationary observer and the particles are oncoming, whereas many other applications use the frame of reference where the observer is moving in a field of stationary particles. In many cases it is conceptually easier to work in the latter frame of reference, which is the approach we will use. Note that relative velocities are reflexive, so the two formulations are equivalent.

The strength of the gas particle model is its wide applicability in many domains. With relatively simple calculations, this model has been adjusted for many different assumptions on the locations and paths of incident and target particles, allowing for relatively flexible applications. More advanced adjustments to the basic model can be used to account for target particle motions, number of dimensions, and relativistic matter/energy considerations in the case of sub-atomic physics.

The gas particle model’s weaknesses for representing encounter scenarios is that it can become difficult to model dynamic situations. Furthermore, the model requires that any object’s motion is independent of the motions of other bodies in the space. No targeting or avoiding behavior is permitted.

1.2.1.3 The Satellite Collision Model

This third model requires more information than either of the previous two. Its primary field of application is in estimating the probability that two satellites

in orbit will collide (Alfano, 2006; Alfriend et al., 1999; Carlton-Wippern, 1993; Chan, 1997). Another common application is in airspace deconfliction by air traffic controllers (Chiang et al., 1997). In both of these cases, there is complete data for estimating positions, velocities, and pairwise covariances of the object motion paths. This model would not work well for predicting interactions where the exact motion paths of the particles are erratic and generally unknown; therefore, it has not been applied to as wide a variety of domains as the other two because of its enormous data requirements.

The collision model requires full information on the perceived location and expected path of every object under consideration. It then uses geometric techniques to compute the points of closest approach for every incident-target object pair. Layering a Gaussian error distribution at the point of closest approach, an upper bound on the probability of collision is estimated by

$$\iiint_V \frac{1}{\sqrt{(2\pi)^3 |C|}} e^{-\frac{1}{2}\bar{r}C^{-1}\bar{r}}$$

where V is the volume of space within which the encounter is expected to occur, C is the combined covariance of the pair of objects and \bar{r} is the collision distance (Chan, 2004).

1.2.2 Discussion

Between these three modeling techniques a large gap exists for encounter scenarios which have data limitations, where encounters are very rare, and where the physical behavior is complex. In this research we will extend the gas particle model with a view towards filling in this gap. Specifically, some examples of scenarios that break the assumptions of existing gas-particle encounter models include:

- Speeds of objects may be dependent on the objects' locations in space

- Objects are not uniformly distributed throughout the space
- The number of encounter-able objects moving in the space is bounded by some positive integer n
- Objects may enter or leave the collision space

1.3 Objective

The goal of this research is to advance encounter model probability theory to provide collision risk estimates for more general spatial and dynamic cases. The sub objectives to be completed are:

1. Research modern point process theory for feasible enhancements to extend the encounter model theory.
2. Apply the enhanced model to a problem scenario to provide a proof of concept for the model.

1.4 Scope

The model developed in this research could apply to a number of different scenarios. The application selected for this research is one of great military interest: a probability estimation that artillery fire may randomly encounter aircraft in midair. Figure 1.1 provides the problem scenario. The artillery unit is firing indirect fires (i.e., the gunner cannot see the target) that arc through an altitude range where aircraft are flying. Clearly such a scenario presents risk to the aircraft, but Musselman (2008) explains further that if pilots are concerned about being hit by friendly artillery fire, they may not be as careful with their munitions as they would otherwise be, since they may be distracted by the extra threat to their aircraft. The threat to aircraft from the ground artillery increases risks for both the aircrews and the ground forces.

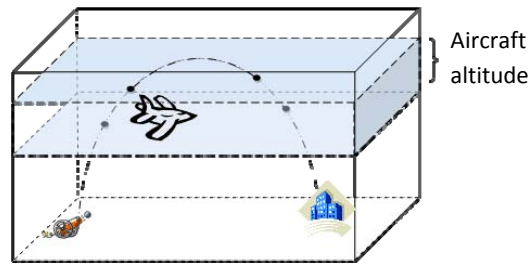


Figure 1 – Problem scenario

Figure 1.1 The Problem Scenario

Current doctrine prevents this from ever occurring by requiring commanders to deconflict the airspace. Deconfliction consists of using fire support coordinating measures (FSCMs) to allocate portions of the airspace for certain use during specified time intervals. Common FSCMs include lateral separation (i.e., you stay on your side of this line, and I’ll stay on my side), altitude separation (e.g. the aircraft flies above the artillery fires), or time separation (JP3-09.3, 2003). The kill box structure is an example of a more complex FSCM that is currently used in military operations (JP3-09.34, 2005).

Despite the fact that joint doctrine requires the application of FSCMs, risk analysis for artillery fires colliding with aircraft in a conflicted airspace is increasingly becoming a point of interest for mission planners, decision makers, and commanders. In December 2007, the Center for Army Lessons Learned published a requirement for an analytical model for assessing the risk of aircraft fratricide due to fires (Neuenswander, 2008). Bethea and Herbranson (2008) point out that several recent exercises on the Korean peninsula highlight the difficulty of deconfliction in small airspaces that are heavily congested. Deconfliction in the Korean peninsula places limits on the commander’s options, ability to mass his forces effectively, and conduct timely responses to new developments on the battlefield. Smith (2006) also identifies that in aerial interdiction operations the FSCMs can provide sanctuary to

the enemy, prevent the prosecution of time sensitive targets, and limit the Commander's and pilot's tactical options.

Under these limitations, the commander is left in a bind where he must choose between one of two options:

1. Accept no risk to aircraft from friendly surface fires by deconfliction. This will result in limitations as described above.
2. Accept an unknown risk that his aircraft will be hit by friendly surface fire by choosing not to deconflict the airspace. This will provide more flexibility since many of the limitations described above are not applicable.

Clearly, an unknown risk makes the decision very difficult to commanders.

There have been two prior efforts at determining this unknown risk. The first was conducted by the National Defense Industrial Association (NDIA) in 2001 (Strike, Land Attack and Air Defense (SLAAD) Committee of the National Defense Industrial Association (NDIA), 2001). Their study was conducted on behalf of the Office of the Chief of Naval Operations. The study covered many aspects of Joint Fires including various methods, tools, and issues with the practice. As a sub-objective, the NDIA team conducted a simulation to test the validity of the "Big Sky – Little Missile" theory that fratricide risks are negligibly small. A number of important details are omitted from the study report, including confidence intervals and numbers of replications of the simulation. However, they conclude that the risk that aircraft will be hit by friendly fire is 1%, which is not a negligible risk. No sensitivity analysis seems to have been performed on the results to test different scenarios.

In 2008 the Air Force Doctrine Development and Education Center (Bethea and Herbranson) started a probabilistic model that reduces the airspace to the vertical plane that cuts through the gun-to-target line (GTL). The plane is then partitioned into aircraft-sized rectangles. The ballistic path is approximated by an

isosceles triangle on the plane. The risk estimate is given by the ratio of rectangles intersected by the triangle to the total number of rectangles. This is a much cruder approximation than we propose to provide with our research.

To date, no published model exists for probabilistic estimation of the dynamic collision likelihood of artillery fires on fixed wing aircraft. Specifically, a model is needed that can account for

- Uncertainty in the artillery location
- Uncertainty in the aircraft location/heading
- Uncertainty in the target location
- Uncertainty in the shell speed
- Uncertainty in the aircraft speed
- Collisions from any possible angle (head-on, from behind, from above, etc.)
- Duration of airspace confliction
- Number of aircraft in the airspace
- Aircraft altitude
- Artillery max ord (highest height achieved by the fired shell)
- Size of the operational area (surface area from a top-down view)

1.5 Overview

Chapter 2 provides a theoretical development of an enhanced gas particle model where the object speeds are spatially determined and their spatial distribution follows a generalization of the spatial Poisson point process. Chapter 3 presents an application of the enhanced model to the proposed study for aircraft fratricides, along with sensitivity analysis and numerical results. Chapter 4 concludes the thesis by highlighting the key research findings and some areas for future research.

2. Theoretical Development

Advancing Encounter Models with Modern Point Process Theory

2.1 Introduction

We consider the general class of encounter models: representations of objects moving in space as they randomly encounter other objects in the space. It is assumed that the space is \mathbb{R}^3 . Common applications of encounter modeling techniques include kinetic theory (i.e., motions and collisions of gas particles) (Brush, 1965), bird strikes (Bird/Wildlife Avian Strike Hazard (BASH) Team, 2008), airspace deconfliction (Alexander, 1970; Pollack et al., 1997), and satellite collision models (Chan, 2004). The result is a more general spatial point process (SPP) which is fully dynamic.

2.1.1 The Difficulty on Dynamic SPPs

Møller and Waagepetersen (2004) define an SPP X on a space $S \subseteq \mathbb{R}^n$ as a measurable mapping on some probability space (Ω, \mathcal{F}, f) to $(N_{lf}, \sigma(\mathcal{N}_{lf}))$ where N_{lf} is the set of locally finite point configurations in S and $\sigma(\mathcal{N}_{lf})$ is its σ -algebra. The distribution of X follows $P_X(F) = P(\{\omega \in \Omega : X(\omega) \in F\})$ for any $F \in \mathcal{N}_{lf}$. They go on to point out that every SPP can be uniquely identified by its corresponding counting process on the collection of closed Borel sets in S , which is the approach taken here. We define a random locally finite point configuration of N points on a set $S \subseteq \mathbb{R}^3$ with the state space

$$\mathcal{B} = \{B_1, B_2, \dots, B_N : B_i \in S\}$$

Then we say that a SPP is binomial if for any $W \subseteq S$, it holds

$$N_X(W) = |W \cap \mathcal{B}| \sim \text{Binomial}(|\mathcal{B}|, f(W))$$

for some density function f on S . Similarly, the Poisson SPP is defined such that for any $W \subseteq S$, $|\mathcal{B} \cap W| \sim \text{Poisson}(\lambda\mu(W))$ and conditional on $|\mathcal{B} \cap W| = N$, the process *inside* W is binomial.

In most applications of SPPs, the points are assumed to be stationary (Møller and Waagepetersen, 2006), which may not be a problem for certain encounter models (see Kim (2002) for example). However, in many encounter scenarios all the particles are in motion, rendering the system dynamic.

The common technique to solve such systems is to change the frame of reference so that only one object is in motion and all the rest are stationary. Loeb (1934) provides a proof that the expected relative velocity, v_{rel} between two objects, A and B , moving in \mathbb{R}^3 , provided that the directions of motion for A and B are independent and at least one is uniformly distributed, is

$$\mathbb{E}_\theta[v_{rel}(v_A, v_B, \theta)] = \begin{cases} v_A + \frac{v_B^2}{3v_A}, & v_A \geq v_B \\ v_B + \frac{v_A^2}{3v_B}, & v_A < v_B \end{cases} \quad (2.1)$$

where v_A and v_B are the speeds of A and B respectively, and θ is the angle between their motion vectors. As a result, the average rate of encounters is increased. Unfortunately, since this is a rate increase it must be evaluated at infinitesimal level. Comas and Mateu in their simulation of a Gibbs process highlight the difficulty of examining such dynamical systems using discrete time-step methods (Comas and Mateu, 2007).

While the Poisson process naturally scales to account for changes at the infinitesimal level, non-Poisson distributions such as the binomial do not scale so easily. Evaluating instantaneous increases in interaction probabilities in non-Poisson spa-

tial distributions is a non-trivial exercise. In fact, if the scaling is attempted in a naive method, it can result in probabilities greater than unity, as will be seen later. Therefore, while quite a few dynamic models exist that employ the Poisson process or its derivatives (specifically the Gibbs process) to examine dynamic encounter systems (Baddeley et al., 2006; Clausius, 1858), to our knowledge no studies have been performed to examine dynamic SPP systems with non-Poisson-based counting processes. Population epidemic models with migration might be considered an exception; however those cases consider migration on a lattice structure rather than in a compact space (Ball and Lynn, 2006; Hagenaars et al., 2004).

2.1.2 The Extended Poisson Process

A natural solution to this problem of infinitesimal estimates on non-Poisson distributions is provided by the extended Poisson process, adapted from the chronological \mathbb{R} domain to the spatial \mathbb{R}^3 domain. The core concept of the extended Poisson process is to use Markov birth-death processes to model counting processes that are over- or under-dispersed with respect to the Poisson distribution. The extended Poisson process uniquely features transition rates that are functionally dependent on the current state. For example, the well known pure birth Yule process is an extended Poisson process with a linearly increasing arrival rate.

The extended Poisson process was developed in the late 1980's through the early 1990's in a series of papers primarily between M. Faddy, F. Ball, and P. Donnelly (Ball, 1995; Ball and Donnelly, 1987; Brown and Donnelly, 1993; Faddy, 1985, 1990, 1994). The culmination of this chain of research was when Faddy showed that any discrete distribution with finite support can be represented by a Markov death process where the transition rates depend on the current state (1998).

Since the discovery of the extended Poisson process, further refinement has been in the realm of advancing statistical data analysis using the extended Poisson process. Parameter estimation techniques for the extended Poisson process model

include maximum log-likelihood calculations for the \mathbf{Q} matrix (Podlich et al., 1999), iteratively re-weighted least squares algorithms (Toscas and Faddy, 2005) and non-parametric sequence algorithms (Podlich et al., 2004). It is interesting to note that Quigley and Walls solve a similar problem where the arrival rate is both dependent on the state of the system (number of arrivals) and the current time by using a bootstrapping technique (2005). In application of statistical analysis, the extended Poisson process has been heavily used in studies of biological processes (Faddy, 1995, 1997; Faddy and Smith, 2008, 2005; Faddy et al., 2001). We are aware of no major further developments of the extended Poisson process as a feature of *probability* theory.

With the bulk of research in extended Poisson processes going into parameter estimation, the application of extended Poisson processes to spatial processes is largely untouched. Faddy performed a short study of spatial data, but overtly bypassed a full development of the formulaic application of the extended Poisson process to the spatial parameters of the problem (Faddy and Smith, 2008). We find, however, that using the Lebesgue measure and integration allows us to easily port the formulas from the time domain to the spatial domain. Most of the key results carry over without any fundamental change. However, in higher-dimensional domains, we find a new usefulness of the extended Poisson process: the ability to smoothly handle increases in rates due to the relative frames of reference used in encounter models.

2.1.3 *Outline*

Section 2 lays the groundwork for our discussion by defining the necessary terminology and assumptions. Section 3 introduces the concept of motion to develop a dynamic SPP. The section concludes with the description of an intuitive step which would seem to allow for estimates of encounter probabilities, but which in fact leads to a paradoxical relationship. The solution is presented in Section 4 with

the introduction of the Extended Spatial Poisson Point Process and an example of the model is presented for a dynamic SPP scenario. Some concluding thoughts are provided in Section 5.

2.2 Definitions, Assumptions, and Scenario Description

We consider the probability that a point A will encounter some point B from a collection \mathcal{B} . Mathematically, the number of encounters is given by a counting process, N_X , on the r -ball of A , $\beta_r(A) = \{s \in S : |s - A| < r\}$ (using the standard $\lVert \cdot \rVert_2$ -norm).

$$N_X = \sum_{B \in \mathcal{B}} \mathbf{I}_{\beta_r(A)}(B)$$

where \mathbf{I} is the indicator function of whether B is in $\beta_r(A)$. Since this counting process is involved, we introduce the following assumption that allows us to apply SPP theory.

Assumption 2.1 *X is a binomial SPP with uniform density function. Thus, if \mathcal{B} is distributed according to X , $|\mathcal{B} \cap W| \sim \text{Binomial}(N, \mu(W)/\mu(S))$, where $N = |\mathcal{B}|$.*

We use the standard Lebesgue measure μ which is assumed to be in 3-space. Later in the development we will require Lebesgue measures in lower dimensions, at which time we will subscript the measure to indicate the number of dimensions.

2.2.1 Defining locations and motion

The core of encounter models is the concept of motion. Motion is commonly known to be the change in position over time. Frequently, the velocity of some object X is denoted by a vector, $\vec{v}_X = (v, \theta, \phi)$, where $v \in [0, \infty)$, $\theta \in [0, 2\pi]$, and $\phi \in [0, \pi]$. Of these, the most important in this paper is the scalar v which we define as follows:

Definition 2.1 *The speed of an object in S is given by \mathbf{v} a mapping $\mathbf{v} : [0, \infty) \rightarrow [0, \infty)$ given by some constant v . The domain is some time duration t , and the image is the measure of some distance, $d = \mu_1[d_0, d_f]$. Thus $\mathbf{v}(t) = vt = d = \mu_1([d-0, d_f])$.*

The above function definition may be read “ d is the distance traveled by moving at speed v for time t .” Note that the restriction to the non-negative reals eliminates consideration of negative times or negative speeds. Throughout this article we will define v as a function space, $s \in S$. Thus, the reader may interpret $v(s \in S)$ as $d = v(s, t) = v(s)t$, which is the distance that would be traveled by moving at speed $v(s)$ for time t .

In the dynamic encounter problem considered here, both A and the elements of \mathcal{B} can be in motion (i.e. have positive speed). Most of kinetic theory literature (hard-body particle collisions on Poisson SPPs) examines cases where the elements of \mathcal{B} have speeds that are independent and identically distributed (see for example Clausius (1858); Maxwell (1858)). To the authors’ knowledge, no prior work exists in the literature that examines encounter cases where the speed of an arbitrary element of \mathcal{B} is a function of the element’s position in S . Examples of this phenomenon abound in the natural environment: traffic lanes have different speed distributions, ballistic projectiles vary their velocity by altitude, aircraft at different altitudes fly at different speeds, and satellite speeds change between apogee and perigee of orbit. Note that in some of these cases the velocities are deterministic and in others they are stochastic in nature.

It would be possible to examine cases where the velocities are random functions of the environment using random fields, but we believe the core concepts can be adequately expressed in deterministic form. Thus, we consider the specific case where the function for speed is deterministic and the direction is uniformly distributed in \mathbb{R}^3 .

Assumption 2.2 *The velocities of all the elements $B \in \mathcal{B}$ are i.i.d. with $\vec{V}_B = (v_B(s), \theta, \phi)$ where $v_B(s) : S \rightarrow [0, \infty)$ is deterministic, $\theta \sim \text{Uniform}[0, 2\pi]$, and $\phi \sim \text{Uniform}[0, \pi]$ (where \sim means “distributed as”).*

Note 2.1 *We recognize that Assumptions 2.2 and 2.1 can place certain limitations on $v_B(s)$ and $X(t)$. For example, the following scenario presents a contradiction:*

$$X(t) = v_B(s) = \begin{cases} 1, & s = s^* \\ 0, & s \neq s^* \end{cases} \quad \forall t \in \Delta t$$

since the system initializes with all elements of \mathcal{B} located at s^ . As the system evolves, s^* is transient, and every other location is absorbing, which contradicts that $B \in \mathcal{B}$ is located at s^* with probability 1. Thus, by the statement of these two assumptions, it is further implicitly assumed that no such contradictions are possible.*

Lemma 2.1 *If B is distributed according to X in S , then the probability that B is in some region $W \subseteq S$ is given by $f(W) = E_W[f(s)] \mu(W)$, where $E_W[f]$ means the expectation of f over W .*

Proof. The result follows trivially from the definition of the expectation:

$$E_W[f] = \int_{s \in W} \frac{f(s)}{\mu(W)} ds = \frac{f(W)}{\mu(W)}$$

■

Having addressed the motion of the elements of \mathcal{B} , we now consider the motion of A , which is intimately related to the encounter region. Since encounters are spatially defined, the occurrence of an encounter depends on the location of the encountering and the encountered. In this problem formulation, A is the encountering object, and the elements of \mathcal{B} are the encountered objects. The locations and motions of the encountered (or unencountered) elements of \mathcal{B} are given by Assumptions 2.1 and 2.2 respectively. We track A 's location by its path as follows:

Definition 2.2 A path, p , is a continuous measurable mapping from $[t_0, t_n] \subset \mathbb{R}_0^+$ into S where $J_p(p(t)) = \vec{v}_A(t)$.

Here $J_p(p(t))$ is the 3-dimensional Jacobian of the path p from A 's location at time t . Definition 2.2 allows for either stochastic or deterministic motion of A . The requirement on the Jacobian limits the path length to what would be achievable with the given velocities:

$$\mu_1(p) = \mu_1 \left(\int_{t_0}^{t_n} \vec{v}_A(t) dt \right) = \int_{t_0}^{t_n} \mu_1(\vec{v}_A(t)) dt = \int_{t_0}^{t_n} v_A(t) dt \quad (2.2)$$

Clearly, in order to define a path $p_A(t)$ according to Definition 2.2, we require the velocity distributions. Previous work assumes that A 's motion is equal in distribution to that of \mathcal{B} . While this is certainly allowable, this is not required by the mathematical formulation of the encounter model. In fact, this model can work for A with *any* distribution on \vec{v}_A (including that of no motion at all). For simplicity we assume that the speed of A is i.i.d. at all moments in time. This means from Equation (2.2) that $E[\mu_1(p)] = E[v_A](t_n - t_0)$. We make no assumptions on the directional components of \vec{v}_A .

Assumption 2.3 $\vec{v}_A(t) = (v_A, \theta(t), \phi(t))$ where $\theta(t) \sim f_\theta(t)$ and $\phi \sim f_\phi(t)$ for some random variables θ and ϕ mapping t to the probability spaces $([0, 2\pi], \mathcal{F}_{[0, 2\pi]}, f_\theta(t))$ and $([0, \pi], \mathcal{F}_{[0, \pi]}, f_\phi(t))$ respectively (where \mathcal{F}_Ω is the Borel σ -algebra on Ω).

2.2.2 Defining an encounter region

Having located A in space, we can now proceed to define the region in which the elements of \mathcal{B} are to be encountered. We do this using a closed ball:

Definition 2.3 Define $\beta_{(d,r)}(s)$ as the closed r -ball of d dimensions ($d \in \{0, 1, 2, 3\}$) at $s \in S$ by $\beta_{(d,r)}(s) = \{s' \in S : \mu(s - s') \leq r\}$ for some $r \in \mathbb{R}^+$

Similarly to the definition of μ , we will forego the use of dimensional subscripts for 3 dimensions. Since $S \subseteq \mathbb{R}^3$ we know that $\beta_r(s)$ is unique. Similarly, $\beta_{(0,r)}(s) = s$ is unique. For $d = 1$ or $d = 2$, $\beta_{(d,r)}(s)$ is not unique in \mathbb{R}^3 . Thus, when we use $\beta_{(2,r)}(s)$ below, we place the further constraint on the 2-dimensional ball that $\beta_{(2,r)}(p(t)) \perp J_p(p(t))$, which makes it unique in \mathbb{R}^3 . For defining the encounter region in \mathbb{R}^3 , the ball definition works for a single point, but since A may be moving in S , we must extend this definition to include all points covered by A during its sojourn along $p(t)$.

Definition 2.4 *Let A move along $p(t)$ for $t \in \Delta t = [t_0, t_n]$. Then let $W_r(p, \Delta t) = \{s \in S : \exists t \in \Delta t = [t_0, t_n] \ni s \in \beta_{(d,r)}(p(t))\}$. We call $W_r(p, \Delta t)$ the encounter window of A along $p(t)$ for $t \in \Delta t$.*

Using the window construct is critical for encounter models. From Lemma 2.1, using $\mu(W_r(p, \Delta t))$, we can find the density function integrated over W , which is used by the binomial process X (given in Assumption 2.1) to compute the random counter of the number of elements in \mathcal{B} encountered by A during Δt .

In order to find W , we break with the standard convention in kinetic theory of using the disks perpendicular to \vec{v}_A , and integrate over the path. Instead, we will use a “leading edge” construct. The result is the same “tube”-shaped encounter window of measure $\mu_d(W) = \mu_{(d-1)}(\beta_{(d-1,r)})\mu_1(p)$ under certain assumptions (see Assumption 2.4 below) on W that prevent it from doubling back on itself with a positive μ_3 measure. We begin by defining the leading edge. The reason for the use of the leading edge as opposed to the disk will be explained at the end of this section.

Definition 2.5 *Let A move along p in S over some time $\Delta t = [t_0, t_n]$. At any time $t \in \Delta t$, let $\mathcal{P}(s)$ denote the plane perpendicular to $\vec{v}_A(t)$ passing through some point s in the image of p . We define the leading edge, $LE_p(s)$, as the intersection of $\beta_r^-(s)$ with the closed half-space bounded by $\mathcal{P}(s)$ and on the same side of $\mathcal{P}(s)$ as $\vec{v}_A(t)$,*

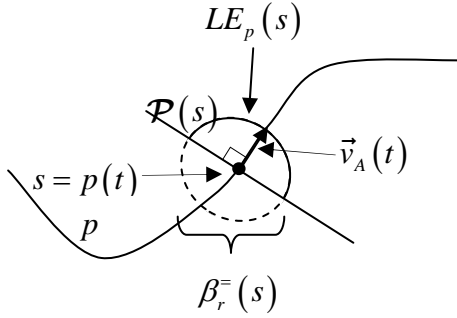


Figure 2.1 The leading edge in 2 dimensions

where $\beta_{(d,r)}^-(s)$ is the boundary of the r -ball given by an equality constraint on the ball definition.

Figure 2.1 gives a 2-dimensional representation of the concept of the leading edge. We constrain the path to prevent the encounter window from doubling back on itself. Clearly, this cannot be done with balls, since the balls for two points $\{t, t+dt\}$ intersect each other at uncountably many points. However, we can achieve the desired constraint using the leading edge.

Assumption 2.4 *If A moves according to path $p \subset S$ over time Δt and the encounter radius is some $r > 0$, then for any $t_a, t_b \in \Delta t$ where $t_a \neq t_b$ it holds that $LE_p(p(t_a)) \cap \beta_r(p(t_b)) = \emptyset$.*

Lemma 2.2 *p is one-to-one.*

Proof. Assume the corollary is false. Then $\exists t_a, t_b \in \Delta t$ where $t_a \neq t_b$, and $p(t_a) = p(t_b)$. Clearly, this would mean $LE_p(p(t_a)) \subset \beta_r(p(t_a)) = \beta_r(p(t_b))$, which contradicts Assumption 2.4. ■

Note 2.2 *It can be shown that Assumption 2.4 holds if p has curvature less than $\frac{1}{r}$.*

Lemma 2.3 *Suppose $|\mathcal{B}| = N$ and the elements B are stationary and distributed in S according to the binomial SPP X . Then let A move along p for some time*

Δt . Suppose further that it is known that for some connected interval, $\delta_1 t \subseteq \Delta t$ with $t_0 \in \delta_1 t$, that $n \leq N$ elements of \mathcal{B} were within radius r from A at some time during δ_1 . Then the probability of encountering further elements in the time interval $\delta_2 t = \Delta t \setminus \delta_1 t$ is given by the formula: $P[N_X(W_r(p, \Delta t)) | N(W_r(p, \delta_1 t)) = n \text{ and } N(S) = N] \sim (\text{Binomial}(N - n, f(W_r^*(p, \delta_2 t))) + n)$.

Proof. Since X is binomial and it is known that $N - n$ elements are contained in $S \setminus W_r(p, \delta_1 t)$, the result follows from the definition of X . ■

Next we consider the *new* encounter region swept by some particle A moving along path p during a connected time interval $\delta t \subseteq \Delta t$. This region is given by $W_r^*(p, \delta t) = W_r(p, \delta t) \setminus \beta_r(p(t_1))$ where $t_1 = \inf(\delta t)$ and if $t_1 \in \delta t$ we exclude the open r -ball, otherwise we exclude the closed ball. Using the leading edge this region is given by the union

$$W_r^*(p, \delta t) = \bigcup_{t \in \delta t} LE_p(p(t)) \quad (2.3)$$

Since this union is incremented as t increases, we refer to it as the *incremental* encounter window.

Our final lemma in this section comes in light of Lemmas 2.1 and 2.3. With the end goal of finding $N_{\mathcal{B}}(W_r^*(p, \delta t))$, from Lemma 2.3 we are required to find $f(W_r^*(p, \delta_2 t))$ which with the help of Equation (2.3) is shown to be

$$f(W_r^*(p, \delta_2 t)) = f\left(\int_{\delta_2 t} LE_p(p(t)) dp(t)\right).$$

This may still be difficult to integrate, but from Lemma 2.1 we can change the right hand side to the product of $E[f(W_r^*(p, \Delta t \setminus \delta_1 t))]$ and $\mu(\int_{\delta_2 t} LE_p(p(t)) dp(t))$. This places us in the position for the final result of this section:

Theorem 2.1 *Suppose A is moving along p for some time δt . Then $\mu(W_r^*(p, \delta t)) = \pi r^2 v_A \delta t$.*

Proof. We know from Equation (2.3) that $\mu(W_r^*(p, \delta t)) = \mu(\int_{\delta t} LE_p(p(t)) dp(t))$.

Then from the properties of the Lebesgue measure μ

$$\begin{aligned}
\mu\left(\int_{\delta t} LE_p(p(t)) dp(t)\right) &= \int_{\delta t} \mu(LE_p(p(t)) dp(t)) \\
&= \int_{\delta t} \mu_2(LE_p^*(p(t))) \mu_1(dp(t)) \\
&= \int_{\delta t} \pi r^2 \mu_1(\vec{v}_A(t) dt) dt \\
&= \pi r^2 \int_{\delta t} v_A \mu_1(dt) \\
&= \pi r^2 v_A \mu_1(\delta t)
\end{aligned} \tag{2.4}$$

where $\mu_2(LE_p^*(p(t)))$ is the surface area of $LE_p(p(t))$ projected onto the plane perpendicular to $\vec{v}_A(t)$, which is a disk of radius r . The projection is necessary because the Lebesgue measure can only be separated into constituent dimensions if those dimensions are orthogonal. ■

It is interesting to note that Theorem 2.1 will also hold if the curvature equals $\frac{1}{r}$ (see Note 2.2), provided certain other conditions hold. The reason is that if the curvature equals $\frac{1}{r}$ the double-counted points have zero measure, since μ is a measure in 3 dimensions. The key is preventing $W_r(p, \Delta t)$ from doubling back on itself with any positive μ_3 measure (i.e., volume). In Assumption 2.4, we required that there are no intersections (even ones of zero measure) since the equality specified there was not in measure, but in the actual spatial points themselves.

We conclude this section by explaining why the leading edge is used as opposed to the more popular disk version. The reason lies in Lemma 2.3. Since we use a general density function f , it is imperative that as A moves forward, we add the proper points, $s \in S$, to the encounter window. The points to add are those on the leading edge. Most of the literature in Kinetic Theory, on the other hand, assumes f is uniform in S , so from Lemma 2.1 it makes no difference which points are added, provided the same volume is added. As seen in Theorem 2.1 the volume added to

the encounter window as A moves forward a certain distance $v_A \delta t$, is equivalent to the volume of a simple cylinder. Therefore kinetic theory prefers the more easily visualized cylinder formed by a disk perpendicular to the direction of motion and integrated over the path.

2.3 \vec{v} as a function of S

The previous section laid ground work by defining bodies, motions, and encounter windows. The focus of this section is to bring all of these together into a single encounter model. Kinetic theory provides a starting point for our development, since much of the work regarding relative velocities has already been done. It is generally known in the field of kinetic theory that the expected relative velocity between two bodies moving according to the Assumptions 2.2 and 2.3, integrated over all possible collision angles in 3-space is given by Equation (2.1) (for a proof see Loeb (1934) or Chapter 3 of this thesis). This result was first published by Clausius (1858) and has been extended in many ways. To the author's knowledge, however, it has never been extended as it is in the following lemma where we allow the speeds themselves to be functionally related to the space.

Lemma 2.4 *If A is moving along $p(t)$ in S at speed v_A , and $B \in \mathcal{B}$ is located in S and moves in random directions with locally defined speeds $v_B(s \in S)$ then the average relative speed between A and B is*

$$\mathbb{E}_S[v_{rel}] = \int_{s \in W} \mathbb{E}_\theta[v_{rel}(v_A, v_B(s))] \frac{f(s)}{f(W)} ds \quad (2.5)$$

where $\mathbb{E}_\theta[v_{rel}(v_A, v_B)]$ is given by Equation (2.1)

Proof. Noting that the probability that B is located at s is $f(s)$, the remainder of the proof follows from the definition of the mean. ■

From the formula of Equation (2.1) and Lemma 2.4, it can be seen that the results are the same if v_A varies over S and v_B is constant. The reason is because the speed of A relative to B is equal to the speed of B relative to A (the velocity simply points in the opposite direction). Thus, our assumptions that v_A is constant and v_B is a function of s is without loss of generality.

This shift in the speed of the encountering particle, A , is of great importance, because velocity is intimately related to distance as seen in Definition 2.1. Since, however, the actual distance covered by A during some time δt is independent of the motion of B (only the *relative* distance), we adopt a new scaled measure that dilates the standard Lebesgue measure, μ_1 , and so accounts for the relative increase in speed.

Definition 2.6 *Suppose Ω is a d -dimensional cube. Define $\mu_{d,rel}^{(\vec{v}_A, \vec{v}_B)}$ as the Lebesgue measure of Ω where the first dimension is dilated by the ratio of the relative speed between \vec{v}_A and \vec{v}_B divided by v_A . Mathematically,*

$$\begin{aligned} \mu_{(d,rel)}^{(\vec{v}_A, \vec{v}_B)} &= \frac{v_{rel}(\vec{v}_A, \vec{v}_B)}{\vec{v}_A} \mu_1(\Omega_{\{1\}}) \mu_{d-1}(\Omega_{\{2,3,\dots,d\}}) \\ &= \frac{v_{rel}(\vec{v}_A, \vec{v}_B)}{\vec{v}_A} \mu(\Omega) \end{aligned} \tag{2.6}$$

where Ω_n refers to the $|n|$ -dimensional cube created by the intersection of Ω and the sub-space of dimensions given in n .

The reason that the dilation is only in the first dimension is because from Definition 2.1 \vec{v} maps to \mathbb{R} , so the dilation due to relative velocity also only occurs in \mathbb{R} . Using the assumption that our measures are in \mathbb{R}^3 , we will use the shorthand $\mu_{rel}^{(\vec{v}_A, \vec{v}_B)}(\Omega) = \mu_{(3,rel)}^{(\vec{v}_A, \vec{v}_B)}(\Omega)$.

Note 2.3 *Suppose A and B are moving in S with speeds v_A and v_B respectively. Then it is easy to see from Equation (2.6) that though the static encounter windows of A and B are different (assuming $v_A \neq v_B$), their encounter windows relative to each*

other are of equal measure. This result leads to the following intuitive expectation for relative encounter windows.

Theorem 2.2 *The expected measure of the new encounter window swept by A relative to a moving B during an infinitesimal time interval $\delta t = (t, t + dt] \subset \Delta t$, conditional on the speeds of A and B, is given by*

$$\mathbb{E}(\mu_{rel}^{\vec{v}_A(t), \vec{v}_B(t)}(W_r^*(p, \delta t))) = \frac{\mathbb{E}[v_{rel}(v_A, v_B)]}{v_A} \mu(W_r^*(p, \delta t)) dt$$

Proof. The proof follows from Equation (2.6) and (2.4)

$$\begin{aligned} \mathbb{E}[\mu_{rel}^{\vec{v}_A, \vec{v}_B}(W_r^*(p, \delta t))] &= \mathbb{E} \left[\frac{v_{rel}(v_A, v_B)}{v_A} \mu(W_r^*(p, \delta t)) \right] \\ &= \mathbb{E} \left[\frac{v_{rel}(v_A, v_B)}{v_A} \pi r^2 v_A |\delta t| \right] \\ &= \frac{\mathbb{E}[v_{rel}(v_A, v_B)]}{v_A} \mu(W_r^*(p, \delta t)) \end{aligned}$$

■

Then by combining Lemma 2.1 with Equation (2.6), we can show a similar property on the f measure of $W_r^*(p, \delta t)$:

$$f_{rel}(\vec{v}_A, \vec{v}_B)(W_r^*(p, \delta t)) = \frac{v_{rel}(v_A, v_B)}{v_A} f(W_r^*(p, \delta t)) \quad (2.7)$$

Which presents us with a dilemma: f_{rel} is no longer a probability measure. Depending on v_A and v_B and $f(W_r^*(p, \delta t))$, it is feasible to generate f_{rel} measures that are larger than unity. Clearly this makes the use of the binomial distribution for the count process of X infeasible.

2.4 The Extended Spatial Poisson Process

The reason that f_{rel} can grow beyond unity is because if motion is possible, it is feasible for a single element $B \in \mathcal{B}$ to exist in two distinct locations in $W_r^*(p, \delta t)$ during the time δt . This would occur when B was discovered at point s at time t , and then it moved to point s' where it was discovered at time t' . However, if we could somehow remove a point from the candidate list of encounter-able elements of \mathcal{B} immediately after it was detected, the problem would be eliminated. The Poisson distribution describes the limiting behavior required here, except that it never changes the arrival rate. Here we use the extended Poisson process with a linearly decreasing arrival rate at each transition, first described by Faddy (1990).

As M. Faddy (1997) explains, a binomial distribution gives rise to the linearly decreasing sequence of arrival rates for a birth-death process: $\lambda_n = -(N - n) \ln(1 - p)$ for $0 \leq n \leq N$. No provision has been made in the literature to allow for inhomogeneity of λ_n , so we will use the expectation of $f(W_r^*(p, \delta t))$ to give us a constant arrival rate over the incremental encounter window.

$$\text{symbol[Arrival rate]}\lambda = -\ln(1 - \mathbb{E}[f(W_r^*(p, \delta t))]) = -\ln\left(1 - \frac{f(W_r^*(p, \delta t))}{\mu(W_r^*(p, \delta t))}\right) \quad (2.8)$$

Then the rate transition matrix of the extended spatial Poisson process corresponding to the spatial binomial process X is given by:

$$\mathbf{Q} = \begin{bmatrix} -N\lambda & N\lambda & 0 & \cdots & 0 \\ 0 & -(N-1)\lambda & (N-1)\lambda & \ddots & 0 \\ 0 & 0 & -(N-2)\lambda & \ddots & 0 \\ \vdots & \vdots & \vdots & \ddots & \vdots \\ 0 & 0 & 0 & \cdots & 0 \end{bmatrix} \quad (2.9)$$

This pure birth processes can be propagated in time using the Chapman-Kolmogorov Forward equations. In the spatial case, we integrate the equations over S instead of

t . Substituting $\mu(W_r^*(p, \delta t))$ in for t in (2.4) of Faddy (1997), and setting the initial condition $\mathbf{p}_0(W_r^*(p, \delta t)) = [1, 0, 0, \dots, 0]$, we will find the probability distribution for the number of encounters in the region $W_r^*(p, \delta t)$, using the formula

$$\mathbf{p}_n = \mathbf{p}_0 \exp(\mathbf{Q} * \mu(W_r^*(p, \delta t))) \quad (2.10)$$

This can be shown to be equal to the binomial distribution $\text{Binomial}(N, f(W_r^*(p, \delta t)))$, where the n^{th} element of \mathbf{p}_n corresponds to the binomial probability of n successes.

Extending Equation (2.10) to the problem where the elements of B are moving we can take two equivalent perspectives to account for the relativity. The first perspective was the one presented previously in Definition 2.6, namely, in order to require the same time to cover the same absolute distance at an increase relative velocity, the Lebesgue measure in the direction of relative motion must be dilated in proportion to the increase in velocity. This would be equivalent in the extended Poisson process to dilating the time t by some proportion. Time dilation is not frequently studied in the area of counting processes. However, the issue of relative speeds and the resultant perception of time or space dilation is extremely important for dynamic spatial processes.

If one prefers to avoid the concept of space or time dilation, an alternative perspective is that there is an *apparent* increase in the number of encounter-able elements in \mathcal{B} . This perspective derives from the fact that the increased number of collisions can come by either increasing the density or inspecting a larger space. Note, however, that the coefficient is applied only to the *remaining* encounter-able elements, thus, the coefficient is placed outside the parenthesis in the elements of \mathbf{Q} .

It can be seen from Equation (2.9) and (2.10), that the effect is the same regardless of which perspective is taken. The exponential term is increased by the coefficient $v_{rel}(v_A, v_B)$, except that in the perspective of increasing the remaining N , the coefficient is buried in \mathbf{Q} .

Example 2.1 *Reversing the roles of A and B, we consider the case where the velocity of A is changing deterministically from the influence of constant uniform acceleration and elements of \mathcal{B} are moving with constant speed in random directions. Recall from Note 2.3 that this formulation is equivalent to the one where v_A is constant and v_B varies by spatial location.*

Let $\vec{v}_A = \vec{v}_0 - gt$ where $\vec{v}_0 = (v_0^x, 0, v_0^z)$ (in Euclidean coordinates), $g = (0, 0, 9.8)$ and $t \in [0, 2v_0^z/g]$. We assume A's path has the starting point $p(0) = (0, 0, 0)$. From this initial condition using the velocities from \vec{v}_A , we get the path

$$p(t) = \left\{ (x, y, z) : x = \frac{2tag}{v_0^z}, y = 0, z = v_0^z t - \frac{1}{2}gt^2 \right\}$$

where $h = (v_0^z)^2/(2g)$ and $a = v_0^x v_0^z/g$. This describes ballistic motion along a parabolic arc from the origin to the point $(2a, 0, 0)$ with zenith $(a, 0, h)$. It can be shown that this path meets the requirements of Assumption 2.4 if $h > r$.

The velocity of A as a function of z is given by

$$v_A(x, y, z) = (v_0^x, 0, (v_0^z)^2 - 2zg) \tag{2.11}$$

for $(x, y, z) : x \in [0, 2a], y = 0, z = h \left(1 - \frac{(x+a)^2}{a^2}\right)$. The incremental encounter window swept by A moving along p has measure (Reese and Sondow, 2009)

$$\mu(W^*) = \pi r^2 \left(\frac{1}{2} \sqrt{a^2 + 4h^2} + \frac{a^2}{4h} \ln \left(\frac{2h + \sqrt{a^2 + 4h^2}}{a} \right) \right)$$

where we use the abbreviated form $W^* = W_r^*(p, \delta t)$. Assuming that X is uniform in S , the probability that a stationary B is in this window is $\frac{\mu(W^*)}{\mu(S)}$.

To make this example more concrete, suppose we start the model with the inputs shown in Table 2.1. From the formulas above, we can tell that the zenith occurs at altitude $h \approx 11.5\text{m}$, the total shot distance is $2a \approx 2 * 30.6$, and the duration of the flight is $t_n \approx 4.1$ seconds. With this information we can be confident that the

Table 2.1 Velocity inputs for example problem

\vec{v}_0	(15 m/s, 0, 20 m/s)
g	9.8 m/s ²
v_B	20 m/s

Table 2.2 Scenario inputs for example problem

S	$[0, 100] \times [0, 20] \times [0, 15] \Rightarrow \mu(S) = 3000m^3$
r	1m
N	4

parameters shown in Table 2.2 for the scenario are reasonably spacious to encompass W^* . They provide a sufficient space to fully contain the collision window.

This gives us a collision window volume of $\mu(W^*) \approx 105m^3$. If we assume that the 4 elements of \mathcal{B} are uniformly distributed in S and stationary, then the density function is for a unit of volume

$$\frac{1}{\mu(S)} \approx \frac{1}{3000}$$

and from Equation (2.8) we compute $\lambda = -\ln(1-f(W^*)) \approx 0.0012$, since $dF(W^*) = \pi r^2 \mu(dp)/3000 \Rightarrow f(W^*) = \pi r^2/3000$. The resultant extended Poisson process \mathbf{Q} matrix then becomes:

$$\mathbf{Q} \approx \begin{bmatrix} -.0042 & .0042 & 0 & 0 & 0 \\ 0 & -.0031 & .0031 & 0 & 0 \\ 0 & 0 & -.0021 & .0021 & 0 \\ 0 & 0 & 0 & -.0010 & .0010 \\ 0 & 0 & 0 & 0 & 0 \end{bmatrix}$$

Now if the elements of \mathcal{B} move at speeds v_B in random directions in \mathbb{R}^3 , we can integrate Equation (2.5) to find the mean relative velocity between A and an arbitrary element $B \in \mathcal{B}$. Since the integration is rather lengthy, we resort to numerical techniques to generate the expected relative velocity.

Numerically integrating with 3 point Gaussian Quadrature (Burden and Faires, 2005) over all altitudes we find that the expected relative velocity for this scenario is approximately 29.92m/s. This means that the average relative velocity between A and some arbitrary element $B \in \mathcal{B}$ is approximately 20% higher than it would be if the B element were stationary. To incorporate the effect of increasing the speed on the collision probability, we can either increase each $(N - i)$ in \mathbf{Q} by 20% or we can increase t by the same proportion. Here we choose to increase $(N - i)$. This gives us a new \mathbf{Q} matrix:

$$\mathbf{Q} \approx \begin{bmatrix} -.0050 & .0050 & 0 & 0 & 0 \\ 0 & -.0038 & .0038 & 0 & 0 \\ 0 & 0 & -.0025 & .0025 & 0 \\ 0 & 0 & 0 & -.0013 & .0013 \\ 0 & 0 & 0 & 0 & 0 \end{bmatrix}$$

Finally, we can exponentiate $\mathbf{Q}\mu(W^*)$ to find the transition probability matrix \mathbf{P}_{ij} :

$$\mathbf{P}_{ij} = \begin{bmatrix} 0.5326 & 0.3622 & 0.0940 & 0.0107 & 0.0005 \\ 0 & 0.6195 & 0.3223 & 0.0549 & 0.0033 \\ 0 & 0 & 0.7298 & 0.2482 & 0.0220 \\ 0 & 0 & 0 & 0.8489 & 0.1511 \\ 0 & 0 & 0 & 0 & 1 \end{bmatrix}$$

We use the initial condition of 0 encounters with $x_0 = [1, 0, 0, 0, 0]$ (alternatively we could use the encounter probability for the ball around the starting position, $\beta_r(0, 0, 0)$), to generate the probability distribution for the number of encounters at t_n , x_{t_n} :

$$x_{t_n} = x_0 \mathbf{P}_{ij} = [0.5326, 0.3622, 0.0940, 0.0107, 0.0005]$$

2.5 Conclusion

In summary, it is clear that the extended Poisson process is applicable to spatial point processes, and can provide significant advances both from a statistical perspective, by accounting for over- and under-dispersed data, as well as the probabilistic perspective, in that it unifies a variety of spatial point processes into one common framework. This framework also has a unique ability to address motions concerns at the infinitesimal level, similar to the spatial Poisson process, while maintaining the features of alternative counting processes. Thus, in the field of dynamic spatial processes, it opens up a whole new horizon of feasible encounter modeling. The applications for such studies include: hard-body collisions in finite particle systems, search and rescue operations, and birth-death processes for links on a mobile ad-hoc wireless networks.

On the other hand, the methods currently in use in spatial process models may provide some insight to advance the theory of extended Poisson processes. To date, the processes are limited in that the rates only depend on the number of arrivals at some time, not the current time itself. Cox and Gibbs processes (Møller and Waagepeterson, 2004) suggest that there may be parallel constructs in the temporal domain to allow for time-variant versions of the extended Poisson process model with time-intransient Markov chains.

3. Case Study

Assessing Probability of Aircraft Fratricide Due to Artillery Fires

3.1 Introduction and Problem Description

The risk analysis for artillery fires colliding with aircraft in a conflicted airspace is increasingly becoming a source of concern for mission planners, decision makers, and commanders. In December 2007, the Center for Army Lessons Learned published a requirement for an analytical model for assessing the risk of aircraft fratricide due to fires (Neuenswander, 2008). Research conducted by the Air Force Doctrine Development and Education Center (Bethea and Herbranson) introduces a probability model that introduces the concept of a shell creating a collision “tube” through the sky with a geometric approximation of the ballistic path. Their model, however, fails to account for the dynamic motions of the aircraft and artillery projectiles. The National Defense Industrial Association (Strike, Land Attack and Air Defense (SLAAD) Committee of the National Defense Industrial Association (NDIA), 2001) also conducts a simulation study that concluded a 1% risk of fratricide. Despite the increase in studies on the subject, no published model exists to date for probabilistic estimation of the risk of fratricide of fixed wing aircraft due to artillery fires.

Figure 3.1 shows a picture describing the problem scenario. Artillery units fire indirectly (ie. the gunner cannot see the target) arcing through an altitude range where aircraft are flying. The model must take into account all the important parameters, but be flexible so that it can operate with minimal information.

The approach to solving this problem begins in Section 3.2 with a literature review on general collision models. The best candidate for solving this problem is selected and adjusted to better match the particular scenario given by this problem.

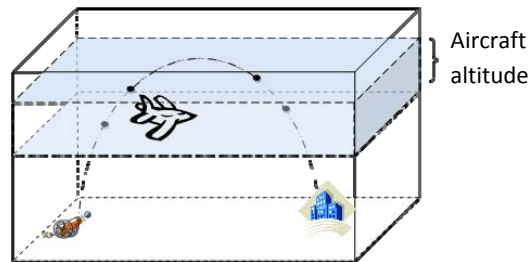


Figure 1 – Problem scenario

Figure 3.1 The Problem Scenario

Specifically, the model is adjusted in Section 3.3.1 to account for ballistic trajectory, spatial M/D/ ∞ birth-death processes in Section 3.3.2, and Section 3.3.3 accounts for uncertainty in the parameters. After these adjustments, the final model represents an original contribution to the literature of collision models. The model is implemented in software and subjected to sensitivity analyses. Finally, numerical results are computed for a simple scenario and some conclusions are drawn.

3.2 *Finding the Right Model*

The issue of things colliding is a point of interest in many different fields of study. The literature is replete with collision studies that represent many different physical collision models with different mathematical bases. Most of these studies seem to solve their respective problem in one of three methods briefly presented here. For further discussion on the models not carried through in this study, see Chapter 1.

1. *The Historical Model:* The general concept is to take historical collision data from similar scenarios, and use these to estimate future collision probabilities. It is a very flexible method that is simultaneously very simple. The drawbacks are finding the data or developing and validating a realistic simulation to generate the data.

2. *The Gas Particle Model:* Here the incident particle moves through space, sweeping through a collision window in the process. Spatial point processes (SPP) provide a probability of a target particle existing in the window. The strength of the model is its wide applicability. Its primary weakness is that it quickly becomes unwieldy and complex when assumptions of independence and uniformity are lost.
3. *The Satellite Model:* This third model uses geometric techniques on location and path information of all objects to compute the points of closest approach for every incident-target object pair. Then it uses a Gaussian error distribution at the point of closest approach to estimate an upper bound on the probability of collision. The strength of this model is its precision, but its weakness is the large data requirements and the probability assumption of normality.

As we consider these three models for use in the problem at hand, we must evaluate their applicability to the problem, flexibility to work under uncertainty, and simplicity of implementation. We quickly reject the satellite model for its data requirements, which greatly exceeds the amount of data that is generally available in real-time combat situations. This presents us with a choice between the historical model and the gas particle model.

The gas particle and the historical models have both been used to develop midair collision estimates. Alexander (1970) uses the gas particle model in estimating the risk of mid-air collisions for aircraft using the “free flight” rules. His “back of the envelope” calculations demonstrate that the gas particle is a viable method of estimating random collisions between particles moving in uncertain directions. The historical model was implemented using simulations by the National Defense Industrial Association (Strike, Land Attack and Air Defense (SLAAD) Committee of the National Defense Industrial Association (NDIA), 2001) to test the “Big Sky – Little Missile” theory for Joint Fire doctrine development. They do not provide

details on the half-width confidence interval results, but report that approximately 1% of their simulated scenarios resulted in a fratricide.

The historical model relies on many past observations of event phenomenon. This technique is not wise to implement in combat theater models apart from simulation. However, in view of the fact that the estimated collision frequency is low, it is reasonable that a simulation approach would require an extensively large simulation time or number of replications to develop sufficiently bounded confidence intervals for realistic results. Nevertheless, Alexander demonstrated that the gas model can be applied to the problem at hand without undue difficulty.

3.3 Model Development

The model is most easily understood in the simpler two dimensional case presented by Kim (2002). Kim examines the probability of activating a mine while traversing a minefield. If a person travels a distance d across the minefield, and he will activate any mines within a radius r , any mines located inside an area of dr will be activated. If the mine density is σ mines per unit area, then the expected number of mines activated will be $dr\sigma$. The aircraft collision model is in 3 dimensions and the artillery shells are in motion, so modifications must be made, but the key concepts are the same. Accounting for the third dimension, the expected number of static fratricides in a collision window swept by the aircraft is

$$\pi r^2 d \sigma \tag{3.1}$$

Visually the model we use here is presented in Figure 3.2. In Section 3.3.1 we use relative velocities to add in motion of the shells. The second step, described in Section 3.3.2, is to estimate the shell density in the collision window by means of a spatial point counting process. Finally, these two results are combined in Section 3.3.3 to give a numerical estimate of the collision risk while accounting for uncertainty

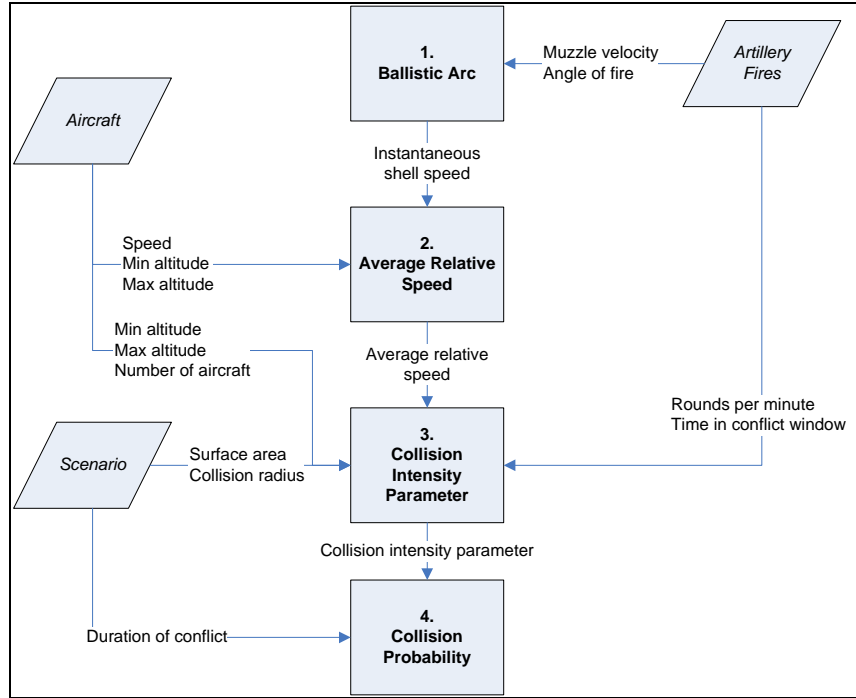


Figure 3.2 Model flow chart.

in the parameters. In forms of calculations similar to the formulas of Kim’s model, the distance d is found in Step 1 of the model and σ is calculated in Step 2.

3.3.1 Step 1: Relative Velocity (Applying Ballistic Formulas)

This collision model deviates from Kim’s minefield model in that the shells are in motion whereas mines are not. Fortunately, Loeb (1934) provides a method to account for shell motion using relative speeds between the aircraft, v_a , and the shell, v_s . Mathematically, this is computed using the Law of Cosines (see Figure 3.3):

$$v_{rel} = c = \sqrt{a^2 + b^2 - 2ab \cos \theta} = \sqrt{v_a^2 + v_s^2 - 2v_a v_s \cos \vartheta}$$

In our problem a and b are the speeds v_a and v_s . ϑ is the angle of incidence between the two motion vectors. The expected relative speed is found by integrating over all possible ϑ angles as follows. We assume that the aircraft path is in some given

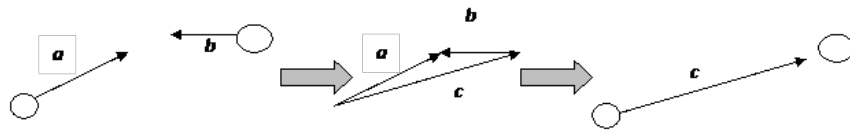


Figure 3.3 The geometry of relative velocities.

direction and that the artillery shell could be coming at it from any direction. Thus, without loss of generality, we fix the aircraft's direction of motion to the vertical axis: $\vec{v}_a = \hat{z}$. Then we assume that the shell's motion vector is uniform in 3-space. If we desire to test whether the angle of approach, ζ is between some angle ϑ and $\vartheta + d\vartheta$, we must take the ratio of the surface area of the "belt" depicted in Figure 3.4 to the surface area of the sphere. If we consider the limiting case as $d\vartheta \rightarrow 0$,

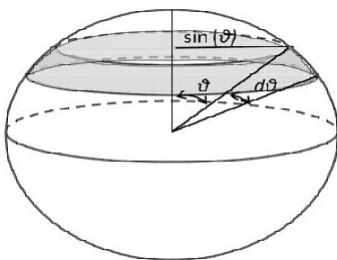


Figure 3.4 Computing the probability of angle of incidence.

the "belt" approaches the side of a cylinder with radius $\sin \vartheta$ and height $d\vartheta$. So the ratio is computed as follows:

$$f(\vartheta) = P(\vartheta < \zeta < \vartheta + d\vartheta) = \frac{2\pi \sin \vartheta d\vartheta}{4\pi} = \frac{1}{2} \sin \vartheta d\vartheta \quad (3.2)$$

We then use the probability of the incidence angle ϑ to find the expected relative speed between two bodies moving in 3 space.

$$\begin{aligned}
E(v_{rel}) &= \int_{\vartheta=0}^{\pi} v_{rel}(v_a, v_s, \vartheta) P(\vartheta < \zeta < \vartheta + d\vartheta) \\
&= \int_{\vartheta=0}^{\pi} \sqrt{v_a^2 + v_s^2 - 2v_a v_s \cos \vartheta} \left(\frac{1}{2} \sin \vartheta d\vartheta \right) \\
&= \frac{1}{6v_a v_s} \left[(v_s^2 + v_a^2 - 2v_a v_s \cos \vartheta)^{2/3} \right]_{\vartheta=0}^{\pi} \\
&= \frac{1}{6v_a v_s} \left[- (v_a^2 + v_s^2 - 2v_a v_s)^{3/2} + (v_a^2 + v_s^2 + 2v_a v_s)^{3/2} \right] \\
&= \frac{1}{6v_a v_s} \left[- ((v_a - v_s)^2)^{3/2} + ((v_a + v_s)^2)^{3/2} \right] \\
&= \frac{1}{6v_a v_s} \left[- |v_a - v_s|^3 + (v_a + v_s)^3 \right] \\
&= \begin{cases} v_s + \frac{v_a^2}{3v_s}, & v_s > v_a \\ v_a + \frac{v_s^2}{3v_a}, & v_s \leq v_a \end{cases} \tag{3.3}
\end{aligned}$$

Note that in Equation (3.3), the speeds are considered constant. However, due to the physics of ballistic motion, shell velocity, v_s , is not constant over the shell's arc. Rather the shell speed decreases as it goes up and increases again as it comes down. In general, v_s is a function of launch angle, θ ; muzzle velocity, v_m ; vertical position, y ; and acceleration due to gravity, the constant g . As an initial model we use the ideal ballistic arc, wherein the instantaneous shell speed at any given altitude follows the equation (for a proof, see Chapter 2)

$$v_s(\theta, y, v_m) = \sqrt{[v_m \cos \theta]^2 + [v_m \sin \theta]^2 - 2yg} \tag{3.4}$$

where θ is the angle of elevation at launch, v_m is the muzzle velocity at launch, g is the gravitational constant (32.2 ms^{-2}), and y is altitude.

Then we set W to be the window volume swept by the aircraft during the conflicted time. If we didn't have relative velocity to consider, we would have $W = \pi r^2 t v_a$. However, we do take the relative velocity into account using Equation (3.3).

Moreover, we also consider the speed of the aircraft at a particular height. Given the launch angle, θ and the muzzle velocity v_m , we combine Equations (3.1), (3.3), and (3.4) to find the new collision window formula:

$$W_{rel} = \int_{t_0}^{t_n} \pi r^2 E[v_{rel}(v_a, v_s(y(t)), \vartheta)] dt \quad (3.5)$$

where $[t_0, t_n]$ is the time that the shell spends in the conflicted airspace.

3.3.2 Step 2: *Shell Density (Applying Spatial Point Process Theory)*

Given the volume W_{rel} , we next count how many shells are actually in the window. The appropriate tool for such a counting process is called a spatial point process (SPP). SPP theory is primarily used for statistical analysis used in areas such as forestry, ecology, seismology, epidemiology and material science (Møller and Waagepetersen, 2006). SPP's come in different variations based on how the points are distributed in space. The Binomial and Poisson distributions are frequently used to model data that is fairly evenly spread out throughout the space. More advanced models such as Cox and Gibbs processes are used if the points tend to cluster together or scatter apart. Rarely do the objects move in any of the models except in two domains: kinetic theory (Brush, 1965) and orbital debris environments (Jenkin and Gick, 2002). In both of these cases, the Poisson SPP is the model of choice because of its memoryless property which creates truly random distributions. In the space/time context the memoryless property is as follows: as I fly through the space, assuming that I do not double back on myself, the number of collisions I've had so far has no bearing on the number of collisions I will have in the future.

We assume that the Poisson process is a reasonable estimate for the shells entering the airspace. This corresponds to an exponentially distributed inter-firing time for the artillery batteries. The assumption of a exponential distribution may seem rather arbitrary, but it is justified on the fact that the distribution is the

most random law that can be used, and so provides a conservative bound on the risk. Furthermore, as the number of artillery units firing into the space increases, Khintchine's (Gross and Harris, 1998) law dictates that the inter-firing times will converge to an exponential distribution.

However, we must also take into account the fact that the shells fly back *out* of the airspace. This requires using a spatial birth-death point process. Since we know from the ballistic arc exactly how long the shell remains in the altitude window, we use a deterministic formula. If an aircraft is flying between altitudes y_{min} and y_{max} , then the duration that the shell spends inside the range $[y_{min}, y_{max}]$ is

$$t = \frac{2}{g} \left(\sqrt{v_v^2 - 2g \min(a_{min}, h)} - \sqrt{v_v^2 - 2g \min(a_{max}, h)} \right) \quad (3.6)$$

where v_v is the vertical component of the muzzle velocity ($v_v = v_m \sin \theta$), $h = v_v^2 / 2g$ is the zenith (henceforth, max ord) of the ballistic arc (again assuming an ideal ballistic arc), and the construct $a_{min/max} = \min\{y_{min/max}, h\}$ handles the cases where the shell falls short of the min or max altitude of the aircraft.

In summary we assume that shells are fired into the space at exponentially distributed time intervals with an average rate λ and that each shell spends the same amount of time in the collision window given by t in Equation (3.6). In queuing theory notation, this is represented as an M/D/ ∞ birth-death process. Adjusting the formulas of Gross and Harris from the M/D/ c queue (Gross and Harris, 1998), the number of shells in the conflicted airspace volume at any point in time is $L \sim \text{Poisson}[\lambda t]$ (\sim means "distributed as"). Thus the number of shells in the whole collision altitude at any given time is found by counting how many shells were fired in the last t seconds. Since L is the number of shells in the whole space, assuming that the shells are uniformly distributed throughout the space, we find the shell density for a unit of air volume, σ by dividing L by the total volume of conflicted

airspace W_T :

$$\sigma_X = \frac{L}{W_T} \sim \text{Poisson} \left[\frac{\lambda t}{W_T} \right] \quad (3.7)$$

Another nice feature of the birth-death process as opposed to other SPP models is that it changes the requirements for the memoryless property. As stated above, the memoryless property requires that the aircraft cannot double back on itself. Clearly this presents a difficulty for estimating fratricide risks for orbiting aircraft. However, with the spatial birth death process, we only require that the aircraft cannot go over its own tracks *inside of t seconds*. Depending on the altitude window that the aircraft is flying in, t is usually no more than only a few seconds – well inside of the time it takes for any aircraft to complete one turn of an orbit.

3.3.3 Step 3: Probabilistic Estimation (Applying Numerical Integration)

We are now able to give a probabilistic estimate of the number of fratricides using Equation (3.1). We substitute Equation (3.5) in for $\pi r^2 d$, and Equation (3.7) in for σ to get:

$$\# \text{ frats} = N_X = \sigma_X * W_{rel} \sim \text{Poisson} \left[\frac{W_{rel}}{W_T} \lambda t \right] \quad (3.8)$$

However, looking back at Equation (3.5), we see that W_{rel} depends on the altitude, y . Similarly t from Equation (3.6) depends on the muzzle velocity, v_m ; the angle of fire, θ ; and the aircraft min/max altitudes, y_{min} and y_{max} . In addition, σ depends on W_T in Equation (3.7). Rarely, however, will the input parameters be known with certainty. It is for that reason that $v_A(y)$ is left in its functional form, since rarely will aircraft fly at one specific altitude. Similarly, it may be reasonable to expect uncertainty in other parameters as well. We expect that W_T , y_{min} and y_{max} will not change over a given altitude, but it is certainly reasonable to expect some variance in v_m , θ , and y .

Considering this, we parameterize the Poisson distribution in Equation (3.8) with

$$\lambda^* = \frac{W_{rel}}{W_T} \lambda t \quad (3.9)$$

and then we make λ^* a function of v_m , θ , and y . Thus Equation (3.8) becomes

$$\# \text{ frats} = N_X = \sigma_X * W_{rel} \sim \text{Poi}[\lambda * (y, \theta, v_m)] \quad (3.10)$$

Then we allow any probability distributions f_{v_m} , f_θ and f_y for their respective variables. For example, we will here use uniform distributions on the launch angle, $\theta \sim \text{Uni}(\theta_{min}, \theta_{max})$; muzzle velocity, $v_m \sim \text{Uni}([v_m]_{min}, [v_m]_{max})$; and collision altitude, $y \sim \text{Uni}(y_{min}, y_{max})$. This allows us to compute the probability for a certain number of fratricides by a conditioning argument

$$\begin{aligned} \text{P}(N_X = n) &= \int_{(y, \theta, v_m)} \text{P}(N_X = n | y, \theta, v_m) \text{P}(y, \theta, v_m) \text{d}(y, \theta, v_m) \\ &= \int_{(y_{min}, \theta, (v_m)_{min})}^{(y_{max}, \theta, (v_m)_{max})} \text{P}(N_X = n | y, \theta, v_m) f(y) f(\theta) f(v_m) \text{d}y \text{d}\theta \text{d}v_m \end{aligned} \quad (3.11)$$

where we know from the Poisson distribution of N_X that

$$\text{P}(N_X = n | y, \theta, v_m) = \frac{e^{-\lambda^*(y, \theta, v_m)} (\lambda^*(y, \theta, v_m))^n}{n!}$$

Since the integral is more complex in this case (considering the amount of computation necessary to find λ^*), we solve it numerically with 3-point Gaussian quadrature. Higher order quadratures provide better estimates, but since multiple integrals are required the number of function evaluations grows exponentially. Therefore the lower order quadrature is chosen for simplicity in this proof-of-concept.

The quadrature technique requires us to build a transformation function t from $[1, -1]$ to the variable domains. So, for a general variable x , we construct the function

$\phi_x(t_x) = t_s \frac{1}{2}(x_{max} - x_{min}) + \frac{1}{2}(x_{max} + x_{min})$ where $t_x \in [-1, 1]$. Then (Burden and Faires, 2005) demonstrates that in the general case,

$$\int_a^b f(x)dx = \int_{-1}^1 f(\phi_x(t_x)) \frac{x_{max} - x_{min}}{2} dt_x$$

We note that the term $x_{max} - x_{min}$ will be canceled out by the f_x terms of Equation (3.11). After these variable shifts, (3.11) becomes:

$$P(N_X = n) = \frac{1}{8} \int_{(t_y, t_\theta, t_{v_m})=(-1, -1, -1)}^{(t_y, t_\theta, t_{v_m})=(1, 1, 1)} P(N = n | \phi_y(t_y), \phi_\theta(t_\theta), \phi_{v_m}(t_{v_m})) dt_{v_m} dt_\theta dt_y \quad (3.12)$$

which is solved using Gaussian quadrature by:

$$P(N_X = n) \approx \frac{1}{8} \sum_{(t_y, t_\theta, t_{v_m}) \in \{-1, 0, 1\}^3} \left(\begin{array}{c} c_y(t_y) c_\theta(t_\theta) c_{v_m}(t_{v_m}) \\ P(N = n | \phi_y(t_y), \phi_\theta(t_\theta), \phi_{v_m}(t_{v_m})) \end{array} \right) \quad (3.13)$$

where

$$c_x(t_x) = \begin{cases} 5/9, & t_x \in \{-1, 1\} \\ 8/9, & t_x = 0 \end{cases}$$

We recognize that Equation (3.13) is daunting to express in a single formula, but it is quite easy to set up using standard spreadsheet software such as Microsoft® Office Excel® (Microsoft® Corporation, 2006). This is the approach we used to perform the sensitivity analysis and to derive the numerical results of the following sections.

3.4 Sensitivity Analysis

Sensitivity analysis was performed on the above model. Figure 3.5 below provides a screenshot of the model implementation in Microsoft® Office Excel®. The data was generally designed to both represent realistic data gathered from Field

Manual 6-40 (HQ , 1999) and Jane’s military resources (Daly, 2008), and to provide insight into the functional relationships represented in the equations. The aircraft speeds and altitudes are generally representative of unmanned aerial vehicles (UAVs) and the muzzle velocities are reduced to highlight functional relationships. Aircraft altitude was represented using a uniform distribution with a spread of 1000 ft. All other parameters are held constant for each observation, and those constants are varied over many observations to generate the output graphs shown.

Comparing muzzle velocity to collision probabilities, until the muzzle velocity attains a critical value, the projectile falls short of the minimum aircraft altitude, and the collision probability is zero. As the max ord gradually travels through the altitude range the collision probability increases until it reaches the maximal value when the max ord equals the maximum altitude for the aircraft. Then the collision probability gradually decreases and levels off at some constant value. The leveling convergence at higher muzzle velocities represents the ballistic path through the at-risk altitudes becoming straighter. As the muzzle velocity increases, the probability converges to the limiting case of the projectile flying through the conflicted altitude in a straight line at an angle equal to the angle of fire. This progression can be seen in Figure 3.6. Since the numerical results match logical outcomes, this serves as validation for the model.

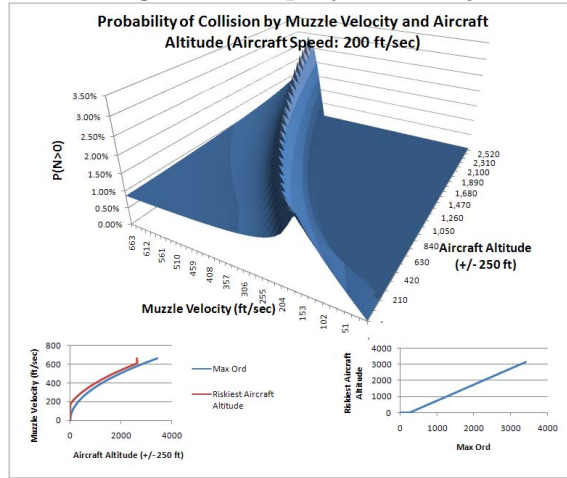
The significance of this relationship between max ord, aircraft altitude, and fratricide risk cannot be overstated. It shows that the point of highest risk is given by a simple linear relationship between where the aircraft is flying and the max ord of the projectile. If the aircraft altitude is $x \pm d$, and the projectile is fired with a max ord of h , then the probability of a fratricide is highest for aircraft flying with an average altitude of $x = h - d$.

The significance of relative velocities is secondary to the muzzle velocity attaining this peak value. This is displayed visually in Figure 3.7. The fratricide probability peaks when the velocity attains the appropriate level for the aircraft

Inputs			
<i>Artillery Unit</i>			
Muzzle Velocity			
Maximum	733	ft/sec	✓
Minimum	732	ft/sec	✓
Angle of Fire (0 = horz, 90 = vert)			
Maximum	41	°	✓
Minimum	40	°	✓
Rounds per minute	2	rpm	✓
<i>Aircraft</i>			
Speed (ground speed)	40	ft/sec	✓
Altitude (Above Ground Level)			
Maximum	101	ft	✓
Minimum	100	ft	✓
Number of aircraft	5		✓
<i>Scenario</i>			
Surface Area	4	nm ²	✓
Min desired miss distance	100	ft	✓
Vulnerable time window	10	min	✓
Outputs			
P(frat) (per aircraft)	197/313	(= 62.94%)	
Collision rate	0.4963045	frats/min	
E(# frats)	4.9630448	frats	
Var(# frats)	4.9630448		
Mean ± 1 St. Dev (# frats during time window)	[0, 0.877]	frats	
N= 0	P(0 frats)=	1/143	(= 0.7%)
Notes			
None			

Figure 3.5 Three groups of input (artillery, aircraft, and scenario) are required to produce an estimate of fratricide along with an uncertainty measure of the estimate.

Figure 3.6 p by v_m and y .



altitude (max ord = $d + x = 250 + 1000 = 1250$ ft, so critical muzzle velocity is approximately 408 ft/sec). Until both the muzzle velocity and aircraft speed reach this critical velocity, changes in aircraft speed minimally affect collision probabilities. As the aircraft speed exceeds the critical velocity, it begins to dominate the equations, so that further increases in aircraft speed drive the probability of collision even higher. Figure 3.8 demonstrates that even the effect of increasing the aircraft speed can be dwarfed by relatively small changes in the collision radius. For example, increasing the miss distance by only 2 ft has about the same impact as raising the aircraft speed by 50 miles per hour.

3.5 Numerical Results

The response values from the model indicate surprisingly high results. A "Big Sky - Little Missile" concept implies miniscule collision probabilities. However, in very normal scenarios here, it is not uncommon for the model to return fratricide risks on the order of 1% to 5%. With input from an experienced Air Liaison Officer (Glen Shilland, 2009), we generated three scenarios presented below. All three have artillery fire with muzzle velocities uniformly distributed between 1525 and 1725 ft/sec and angles of fire uniformly distributed between 35 and 45 degrees. These

Figure 3.7 p by v_m and v_a .

Probability of Collision by Muzzle Velocity and Aircraft Speed (Aircraft altitude: 1000)

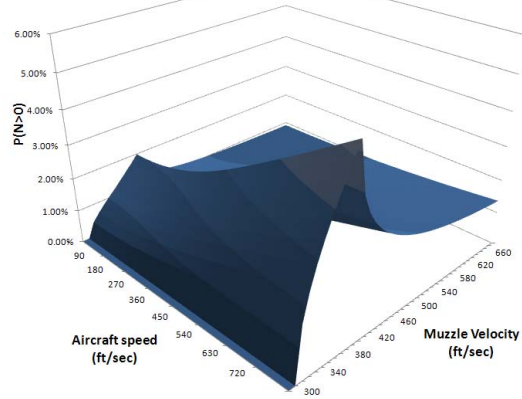
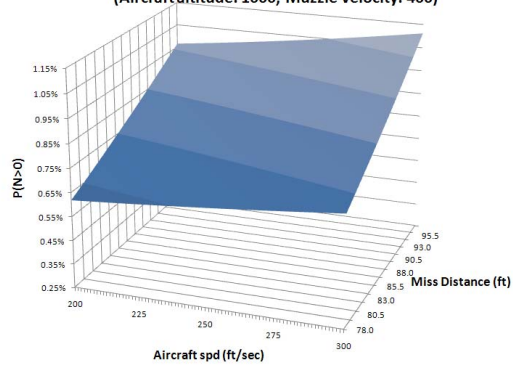


Figure 3.8 p by v_a and r .

Probability of Collision by Miss Distance and Aircraft Speed (Aircraft altitude: 1000, Muzzle Velocity: 400)



ranges correspond to a minimum distance to target of about 20 km and a maximum of about 28 km. The targets are uniformly distributed throughout surfaces areas (ie. a top down view) called grid squares. Each grid square is 1 km^2 . Since the target areas are so much smaller than the distances from the artillery to the target, we assume that the shells only pass through the altitudes on descent, so t in Equation (3.6) does not have the 2 coefficient.

3.5.1 Scenario 1

Our first scenario was intended to be conservative. The artillery is firing at a target in 1 grid square at a rate of 2 rounds per minute (rpm). Meanwhile a 2-ship flight of A-10s attack the target. The A-10s fly at 330 knots (kts) between 4500 and 5500 ft above ground level (AGL), proceed directly above their target, and fly out of the grid square. The entire duration of the conflicted airspace is 6 seconds (the approximate time it takes to cross a grid square at 330 kts). We desire the probability that any rounds pass within 50 ft of the center of either aircraft.

The result of the scenario is that there is less than 0.001% risk to each aircraft. Overall, the probability that no shells pass within 50 ft of either aircraft is approximately 99.95%, or alternatively stated, there is a 0.05% risk that a round will pass within 50 ft of at least one aircraft. This is a very low risk, however, the results can be very sensitive to the radius of collision. Figure 3.9 displays the effect of increasing the minimum desired miss distance on the probability of a shell passing within the radius of either aircraft.

3.5.2 Scenario 2

The second scenario considers the same artillery barrage on the target inside of 1 grid square. This time, 2 RQ-7A Shadow unmanned aerial vehicles (UAVs) are in orbit gathering intelligence on the battle development. They are flying at 75 mph between 4800 and 5200 ft AGL. The entire scenario lasts 10 minutes, and it is again

Figure 3.9 Comparing the probability of no fratricide to collision radii

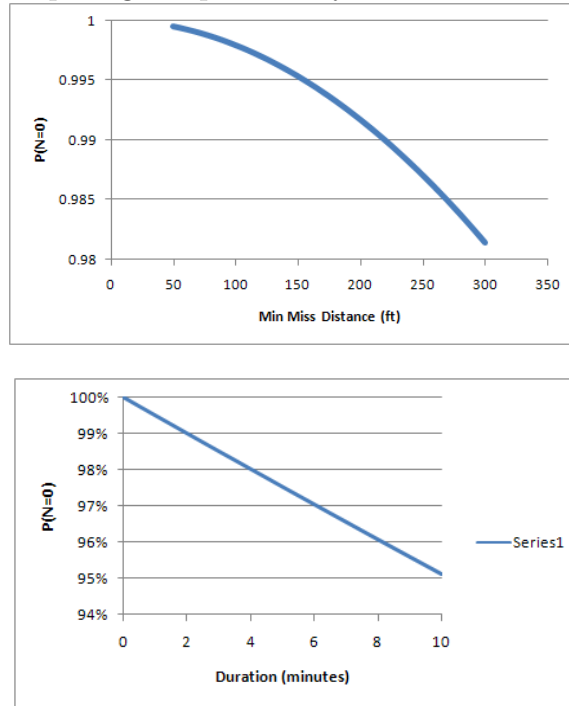


Figure 3.10 Comparing the probability of no fratricide to scenario duration

desired to know the probability that any rounds pass within 50 ft of the center of either aircraft.

This scenario results in a much higher risk: a 4.87% risk that at least one shell will pass within 50 ft of one of the UAVs. Each UAV individually has a 2.46% risk. The major reason for the increase in risk from the last scenario and this one is the duration of the airspace conflict. We show the effect that duration has on the risk in Figure 3.10.

3.5.3 Scenario 3

Our last scenario was intended to examine a more congested airspace. This scenario increases the firing rate to 5 rpm, but also spreads it out over 4 grid squares. The result of this is that the density is reduced by .75 rounds per grid square per minute. In this scenario 2 helicopters are orbiting the area between 1900 and 2100

ft AGL at 100 kts, 2 UAVs are on surveillance flying at 55 kts and 4800 to 5200 ft AGL, and 2 A-10s are on orbit for CAS support at 9500 to 10000 ft AGL and 250 kts. The minimum desired miss distance for all aircraft is again 50 ft.

Individually, the aircraft have fairly decent probabilities of no fratricides: the helicopters have a 99.51% chance of no shells, the UAVs have 98.40% chance, and the A-10 planes have a probability of 97.94% chance of both being at least 50 ft from any shells. However, collectively, there is a 5.06% chance that the center of at least one of these aircraft will be within 50 ft of some shell.

3.5.4 Further discussion

These probabilities are of sufficient risk to warrant attention. In comparison, if a 0.1% risk of incapacitation is presented to ground troops supported by artillery fire or close air support, the situation is termed “Danger Close,” which requires that the “supported commander must accept responsibility for the risk to friendly forces when targets are inside the [danger close zone].” (Joi, 2003). In the second and third scenarios, the risks are 50 times as large as the “Danger Close” threshold.

Furthermore, when considering the expected costs of flying through conflicted airspaces, the results are frequently non-trivial. Not considering the probability of kill (p_k) values, the 0.05% risk to an A-10, priced at 12 million, corresponds to an expected cost of the mission of \$60,000. These are just the “nuts and bolts” costs and do not include effects such as unit morale degradation, loss of public opinion, reduced of mission effectiveness until repairs, or medical costs. Most of such missions through conflicted airspaces will not realize such costs, since the probability of safe passages are so high, but it would not be wise to ignore such non-trivial risks with such large consequences.

These numerical results suggest that the current military policy on deconfliction of aircraft and artillery fire is a prudent course of action. The high expected cost of flying through artillery fires must be matched by an even higher expected gain

in order for the mission to be worth the possible loss. Furthermore, given current stand-off firing capabilities and high altitude ISR, it may be possible to adjust flying missions to achieve deconfliction with minimal degradation of the desired mission effect. Decision analysis can aid planners in trade-off analysis for specific scenarios given the probability calculations presented in this paper, but in general, this model indicates deconfliction is the recommended course of action.

3.6 Conclusion

Despite the many collision models presented in the literature, the gas model is the best probabilistic model for addressing the problem of aircraft fratricides from artillery fire. It provides good fidelity with low data requirements. The adjustments that are necessary to apply the gas model to the fratricide problem require mathematical contributions from diverse fields. Adjusting the “minefield” model to account for three dimensions, non-constant shell velocity that follows ballistic equations, and integrating for uncertainty in the input parameters all combine to form a unique model that provides an original contribution to the literature of collision models.

Numerical results from the model indicate unexpectedly high collision probabilities in normal scenarios. Deconfliction is a prudent response to mitigate the expected costs to joint campaigns, but decision analysis tools may be necessary in certain situations to evaluate the best course of action. Sensitivity analysis on the model serves the dual purpose of providing validation for the model and simultaneously suggesting options for lowering collision risks.

There are several areas where this collision model can be improved. First, the unexpectedly high collision probabilities suggest that a simulation model could reasonably provide further validation of the model without running the risk of poor estimates resulting from rare occurrences due to tail probabilities. Better ballis-

tic models that incorporate drag coefficients may provide better estimates, but the marginal improvements in accuracy may be outweighed by the increase in complexity. Finally, the model could be expanded to include location on the artillery unit, target, and/or aircraft position using inhomogeneous intensity parameter values.

4. Conclusion

4.1 *Research Summary*

This thesis developed a useful extension to the gas particle collision model. It demonstrated the feasibility to account for spatial dependencies in the object velocities. In addition, the extended Poisson SPP allows the analyst to compute collision probabilities when the density of objects in a bounded space may be over- or under-dispersed with respect to the Poisson distribution. This even allows for binomial or negative binomial SPPs. Finally, multi-dimensional birth-death processes allow the modeler to represent objects entering and exiting the space. Each one of these enhancements presents an original contribution to the literature of encounter models.

The application of the research to the problem of aircraft fratricides from artillery fire provides an excellent forum to test the capabilities of the model. Validation via sensitivity analysis suggests the model is accurate. The application provides useful insights to the problem domain that can affect military policy and doctrinal decisions.

4.2 *Future Work*

Recent theoretical development for encounter models is limited. For dynamic situations, the literature is limited to three-dimensional cases. This is probably due in no small part to the difficulty in evaluating the probability density function for the collision angles in other dimensions. The three dimensional case can be solved with simple u substitution, as shown in Chapter 3. However, there are many applications that could benefit from an encounter estimate for a dynamic two-dimensional model. Higher dimensional models may also be useful, though their applications may be more limited. Of particular interest is the case in dimensions higher than eight. This is because it has been shown that the surface area of a unit hypersphere is maximal

in seven dimensions (among integer dimensions) (Weisstein, 2009). For dimensions greater than seven, the surface area monotonically decreases. This may have some interesting effects on the probability of the angles between different motion vectors according to the development in Chapter 3.

Another theoretical development that is still lacking in the literature of encounter models is that of inhomogeneous spatial distributions. Mathematically this would probably entail some sort of Gaussian distribution around the expected location of the object at any given time (Fraser, 1951). Naturally, this must also take into account the probability density function of motions of the objects. If the objects move in uniformly distributed directions, any inhomogeneities in the SPP density function will dissipate as the system evolves. One means to maintain the spatial inhomogeneities would be to model the point arrivals using the spatial birth-death process and distribute the arrivals using a Wiener process for the time since their arrivals. Similar techniques may also assist in estimating uncertainty in the defined motion paths of the encounter-*er*.

The application presented in Chapter 3 may be improved by allowing inhomogeneous spatial density functions. This would reflect more realistic conditions where there is a higher probability of shells or artillery to exist in certain regions (i.e., along the gun-to-target line, or in a particular orbit). As stated in the previous paragraph, this would necessitate further consideration on the assumption of uniformly distributed directions of motion.

The insight that collision risks are non-negligible highlights the need for optimization techniques to optimize the management of a congested airspace to allow for maximum mission effectiveness with minimum risk. This may involve optimization methods to deconflict the airspace. Alternatively, it may be desirable to assign motion paths through a conflicted airspace that travel to designated destination points with minimal risk of fratricide.

Finally, the model described here can be applied to a number of other problem scenarios other than the one described in Chapter 3. One application would be dynamic spatial birth-death systems that represent mobile ad-hoc wireless networks. Since wireless signals require spatial locality to maintain sufficient strength, it would be of interest to know the probability of a particular node going out of signal range, or simply dropping off the network. The implications of such estimates may assist in developing robust policies for network information flow that can maximize the probability that certain packets can reach certain nodes.

Appendix A. Blue Dart

Foregoing Deconfliction: Consider the Risk!

Capt Timothy Holzmann and Dr. Jeffery Cochran

Dept. of Operational Sciences

Air Force Institute of Technology

Integration of air-to-surface fires and surface-to-surface indirect fires requires application of appropriate restrictions: altitude, time, or lateral separation – (JP 3-09.34)

“From Deconfliction to Integration to Interdependence!” is the current mantra. Current operations tempos are driving commanders to make “Go” or “No Go” decisions in very short amounts of time, while simultaneously increasing joint operational effectiveness by having all service branches work together to achieve a synergistic effect. For example, a commander may want Army artillery and Air Force close air support to work together against some target. This naturally may present a risk to the aircraft if it were to fly in the path of an artillery shell. In the military world, taking unnecessary risks can lead to deadly consequences.

Joint doctrine requires commanders to eliminate the risk that the artillery will accidentally hit the aircraft by instructing military planners use deconflict the airspace: designate separate times/places for the artillery units to shoot and the aircraft to fly (Joint Publication 3-09.3). However, recent military operations in Iraq, Afghanistan and exercises on the Korean peninsula have highlighted several drawbacks of requiring deconfliction. It can (1) limit the commander’s ability to respond in a timely manner, (2) prevent him from massing his forces effectively, (3) limit the pilot’s tactical options, (4) provide sanctuary to the enemy, and (5) hinder the prosecution of time sensitive targets. The commander is left in a bind: accept no risk by deconflicting and accept these limitations, or avoid the limitations but accept an unknown risk by flying our aircraft through our own artillery fire. Should

a commander take the risk? Can he count on the “Big Sky - Little Missile” theory to come through, or should he bet on “Murphy’s Law” that something will go wrong?

In 2001, the National Defense Industrial Association (NDIA) performed a study to test the “Big Sky - Little Missile” theory using a series of simulations (Integration, Control and Deconfliction of Joint Fires Study, Volume 1). Their simulations of 4 aircraft flying through a barrage of artillery fire generated only 1% collision probabilities. They conclude: “Chance for conflict still a risk though probability low.”

More recently we teamed up with the Warfighter Applications team from the Air Force LeMay Center to build mathematical formula for the question of ground-to-air fratricide risk. Simulations can vary results from one run to the next, whereas a formula never changes its answer. However, mathematical models are frequently much harder to construct. In this case, the calculations involved ranged from high school physics formulas to graduate school mathematics. The Air Force Studies and Analyses agency provided preliminary review and validation of the model. After further consultations with experienced military operators, our AFIT team generated several realistic scenarios involving close air support operations and unmanned aerial vehicle surveillance operations. Their results indicated that collision probabilities for very normal situations can range up to 1% to 5%. While risk values depend greatly on the particular scenario, both the NDIA and AFIT studies show that they are frequently higher than what might be assumed under the “Big Sky - Little Missile” theory.

Probabilities must be multiplied by the high price tags of modern aircraft to generate the expected cost. Flying a \$12 million aircraft, such as the A-10 Warthog, through artillery fire at 1% chance of it getting hit is like throwing away \$120,000 - and that’s not counting loss of public confidence or a pilot’s life. Furthermore, what would the loss of that A-10 mean to the unit’s effectiveness until it could be replaced? As one former A-10 pilot stated, “It is one thing to be crawling around in

the mud with the infantry when some other pilot accidentally gets shot down by US artillery; it is quite another to be the pilot who has to walk home” (Capt. Hensley, “A Fly Paper”).

We cannot turn these decision processes into just a game of numbers. Finding a numerical risk value is easy compared to shouldering the responsibility of the consequences. However, we can take a cue from the quantitative estimates: the numbers suggest that the current policy of deconfliction is a prudent course of action.

Every day letters are going home to mothers, fathers, wives, husbands, and children expressing our regret on the part of a grateful nation for the sacrifices of brave members of our armed forces. The hardest ones to write are those when we killed one of our own.

Probabilistic Estimation of Rare Random Collisions in 3-Space



Capt. Timothy Holzmann
Advisor: Dr. Jeffery Cochran
 Department of Operational Sciences (ENS)
 Air Force Institute of Technology

Objective Statement

Advance encounter model probability theory to provide collision risk estimates for more general spatial and dynamic cases.

Application Domains

- Risk analysis for flying fixed wing aircraft traversing airspace that has not been deconflicted with ground artillery fires
- UAV collision probabilities
- Search and rescue operations
- Reachability probability for mobile ad-hoc networks

Research Results

- Developed model for collision estimation of artillery fires on fixed wing aircraft
- Debunked "Little missile – Big Sky" theory: the risk can be significant!
- Technical contributions to the literature:
 - Dynamic point process models
 - Spatially dependent velocities,
 - Extended spatial Poisson process

References

Betha, D., & Hebranson, T. (2008, July 25). "Calculating the Number of Aircraft Volume Boxes Hit, Within A Certain Airspace, By a Ballistic Following A Simple Trajectory." Maxwell AFB, OH: Personal communication.

Faddy, M. J. (1997). "Extended Poisson Process Modelling and Analysis of Count Data." *Biometrical Journal*, 39, 43-44.

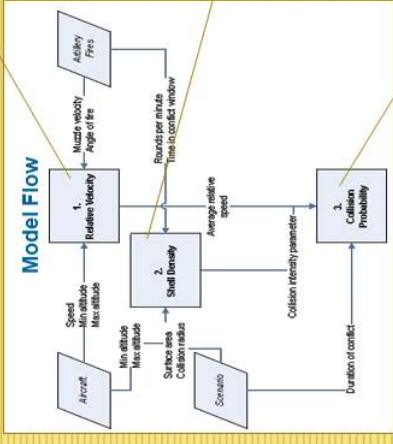
Leeb, L. B. (1934). *The Kinetic Theory of Gases*. New York: McGraw-Hill Book Company, Inc.

Møller, J. and Waagepetersen, R. P. (2006). "Modern Statistics for spatial point processes." *Scandinavian Journal of Statistics*, 34, 643-684.

Shick, L. and Atchick, A. (2005). "Committee on Integration, Control and Detection of Air Defense Fires Study." Volume 1. Arlington, VA: National Defense Industrial Association, February 2001, 81.

Research Partners:

- AFW/Lemay Center
- AF/A9 Studies, Analysis, & Lessons Learned
- Army TRADOC/CDID



Inputs	
Artillery Unit	
Muzzle velocity	
Maximum	1715 ft/sec
Minimum	1515 ft/sec
Angle of fire (0 = horiz; 90 = vert)	
Maximum	45
Minimum	35
Bounds per minute	2
Aircraft	
Speed (ground speed)	110 ft/sec
Altitude (Above Ground Level)	
Maximum	5200 ft
Minimum	4800 ft
Number of aircraft	2
Scenario	
Surface Area	
Min desired miss distance	0.3 ft ²
Maximum	50 ft ²
Vulnerable time window	10 min
Output	
Ft/frats (per aircraft)	17/660 (≈ 2.46%)
Collision rate	0.0049891 frats/min
Ft/frats	0.0498913 frats
Var (ft/frats)	0.0498913 frats
Mean ± 1 St. Dev	(0, 0.877) frats
Std	0.936 frats
90% CI	(0, 1.863) frats (≈ 0.13%)
95% CI	(0, 2.46%) frats

1. Relative Velocity

Relative velocities allow us to change the frame of reference so that one of the objects is stationary

The expected relative velocity is found by integrating over all possible collision angles.

$$f(\phi) = \lim_{N \rightarrow \infty} \frac{1}{N} \sum_{i=1}^N \sin^2 \phi_i$$

2. Shell Density

Kinetic theory uses exclusively spatial Poisson counting processes, which allows for arbitrarily many points in a bounded region.

Encounter models frequently limit the number of encounterable entities in the space

$$Q = \begin{bmatrix} -N\lambda & N\lambda & 0 & \dots & 0 \\ 0 & -(N-1)\lambda & 0 & \dots & 0 \\ 0 & 0 & -(N-2)\lambda & \dots & 0 \\ \vdots & \vdots & \vdots & \ddots & \vdots \\ 0 & 0 & 0 & \dots & \lambda \end{bmatrix}$$

The extended Poisson process enables Markov counting processes to include finite binomial distributions.

3. Collision Probability

Numerical integration used to integrate over multiple altitudes

Results propagated through time with the Chapman-Kolmogorov forward equations.

Sensitivity analysis indicates risk is highest for ballistic arcs that have a zenith at the maximum altitude of the aircraft flight plan

Numerical analysis indicates that military scenarios can have risks up to 1%-5%!



Appendix C. Excel Model User Guide

The software implementation is in the form of a Microsoft® Office Excel® spreadsheet Microsoft® Corporation (2006). There are three separate worksheets within the file label “Start Here,” ”Inputs & Outputs”, and ”GaussQuad” respectively. Each of these three worksheets is treated below.

C.1 Worksheet 1: “Start Here”

The intent of the software tool is to present the minimum level of complexity required for an analyst to perform the necessary calculations and find the desired results. This first worksheet provides the most simple presentation. The worksheet is divided into several regions: the model calculator, the converter, the data suggestions, and the charts.

C.1.1 The Model Calculator

The calculator is the main area of user interface. There is an input section, an output section, and a notes section. Each of these is explained below. Figure C.1 displays these three sections as they are laid out in the software tool. The units for each measure, whether input or output, are designated beside the appropriate cell. Cells intended for user input are colored white, cells with calculated values have a light shade, and the other cells have a darker shade.

The inputs are grouped by the component of the scenario that the respective parameters describe. The artillery section requires the muzzle velocity, angle of fire, and the number of rounds per minute that the artillery unit will be firing. As a simplifying feature, the model eliminates the need for further inputs by assuming that the standard conditions of the U.S. Army field manual 6-40 applies HQ (1999). These conditions are reproduced in Figure C.2. In addition, the model assumes that there is no drag on the projectile, so the shell follows an ideal ballistic arc. Aircraft

Inputs				
<i>Artillery Unit</i>				
Muzzle Velocity				
Maximum	733	ft/sec		✓
Minimum	732	ft/sec		✓
Angle of Fire (0 = horz, 90 = vert)				
Maximum	41	°		✓
Minimum	40	°		✓
Rounds per minute	2	rpm		✓
<i>Aircraft</i>				
Speed (ground speed)	40	ft/sec		✓
Altitude (Above Ground Level)				
Maximum	101	ft		✓
Minimum	100	ft		✓
Number of aircraft	5			✓
<i>Scenario</i>				
Surface Area	4	nm ²		✓
Min desired miss distance	100	ft		✓
Vulnerable time window	10	min		✓
Outputs				
P(frat) (per aircraft)	197/313	(= 62.94%)		
Collision rate	0.4963045	frats/min		
E(# frats)	4.9630448	frats		
Var(# frats)	4.9630448			
Mean ± 1 St. Dev (# frats during time window)	[0, 0.877]	frats		
N= 0	P(0 frats)=	1/143	(= 0.7%)	
Notes				
None				

Figure C.1 A screen shot of the Excel model

STANDARD CONDITIONS	
1	WEATHER
2	AIR TEMPERATURE 100 PERCENT (59°F)
3	AIR DENSITY 100 PERCENT (1,225 gm/m ³)
4	NO WIND
POSITION	
1	GUN, TARGET, AND MDP AT SAME ALTITUDE
2	ACCURATE RANGE
3	NO ROTATION OF THE EARTH
MATERIAL	
1	STANDARD WEAPON, PROJECTILE, AND FUZE
2	PROPELLANT TEMPERATURE (70°F)
3	LEVEL TRUNNIONS AND PRECISION SETTINGS
4	FIRING TABLE MUZZLE VELOCITY
5	NO DRIFT
LEGEND: gm/m ³ – grams per cubic meter	

Figure 7-1. Standard Conditions.

Figure C.2 Excerpt from FM 6-40 containing standard firing conditions

are described by their altitudes, speed, and quantity. The scenario specifications include the size of the operational area (ie. a top-down view of the area where the aircraft are flying and artillery are firing), duration of the airspace confliction, and the minimal desired miss distance. All inputs have a “sanity check” beside them which is green if the parameter is within allowable constraints, yellow if it is on the border, and red if it is outside allowable constraints. For example negative values will be marked red. These flags are also highlighted in the notes section below.

The inputs for angle of fire, muzzle velocity, and aircraft altitude are required in ranges. The actual values will be assumed to be uniformly distributed over the specified ranges. Ranges must be of positive length (ie. max must be greater than the min) or else the calculator will provide erroneous results.

The outputs of the software model (seen in the middle box of Figure C.1) include a probabilistic assessment of the risk of one or more collisions during the conflicted time period. This is the basic computational result from Chapter 3. In addition, the model provides the rate at which collisions are expected to occur, the expected number of collisions over the whole scenario, and its variance. Since variance is difficult to interpret to a operational community, a range estimate is also provided that gives reasonable upper and lower bounds on the expected number of collisions during the given time period. Finally, a binomial distribution is used to

test the probability that a given number of fratricides (up to the number of aircraft) will occur.

The notes section flags important notes to the analyst on the whole scenario. Specifically the calculations are made from considering 9 different combinations of possible angles of fire and muzzle velocities. The notes section flags to the user cases where the projectile fails to reach the minimum and/or maximum altitudes at which the aircraft are flying. If it fails to reach the minimum altitude, the probability of collision is zero. If it fails to reach the maximum altitude, the probability may be also reduced from the case where it passes through the full range going up and coming back down.

C.1.2 The Unit Converter

Also provided for the user are a unit conversion table to aid the analyst in deciding the right inputs. This converter, shown in Figure C.3, is displayed just to the right of the model calculator. The first two sections of the converter will calculate the appropriate muzzle velocity of artillery fire for a given angle of fire and distance to target; and it will calculate the appropriate angle of fire for a given muzzle velocity and distance to target. Below this are various unit conversions with the units specified.

C.1.3 The Data Suggestions

The default data, as seen in Figure C.4, gives the user some reasonable inputs for aircraft velocities and altitudes. The data provided is unclassified, gathered from Jane's military resources Daly (2008), and Wikipedia Wikipedia Contributors (2009a,f,e,b,c,d). The intention is to make the model simple to use for the average analyst.

Useful calculations	
Find Artillery Velocity	
Distance to target	25km
Angle of fire	45degrees
Muzzle velocity	1625.129ft/sec
Find Artillery Angle	
Distance to target	10km
Muzzle velocity	1625.129ft/sec
Angle of fire	11.78909degrees
Conversions	
<i>m² --> nm²</i>	
1miles ²	= 1.324341nm ²
<i>miles --> ft</i>	
0.060386miles	= 318.8406ft
<i>ft --> miles</i>	
4921ft	= 0.932008miles
<i>knots --> ft/sec</i>	
330knots	= 556.9758ft/sec
<i>mph --> ft/sec</i>	
75mph	= 110ft/sec
<i>mils --> degrees</i>	
1200mils	= 67.5°
<i>meters -->ft</i>	
4000meters	= 13123.2ft

Figure C.3 The conversion table

Baseline Aircraft Data				
Type	Aircraft	Speed (mph)		Cruise alt
		Cruising	Maximum	
Tactical	A-10	340	518	
	F-15		900	
	F-16		1320	
	F-22		1043	
Cargos	C-17		403	
	C130		400	28000
	RQ-7A Shadow	75	141	
	Silver Fox	81		12000
UAVs	FQM-151A Pointer	22	56	12500
	AV RQ-11 Raven	40	60	100
	RQ-1 Predator	84	138	25000

Figure C.4 Table of Baseline Data

C.1.4 Graphs

The graphs provide the analyst with an understanding of how the risk varies over various uncertainties in the input parameters. All three graphs plot the surface of the probability of no collisions against angle of fire and muzzle velocity. They differ in the altitudes at which the calculations are made. Collectively the three graphs show the surface over the full range of uncertainty in the inputs.

C.2 Inputs & Outputs

The second worksheet gathers the inputs from the first page in a unified form. It performs range checks on the inputs to ensure that they meet the range requirements. It also collects the results data from the third worksheet and performs basic calculations to prepare them for output to the first worksheet.

C.3 GaussQuad

The final worksheet performs the Gaussian Quadrature calculations specified in Chapter 3 of this thesis. Table C.1 outlines the role of each column in computing the numerical integration. Figure C.5 gives a screenshot of the worksheet.

Table C.1 Clarification on column meanings for “GaussQuad” worksheet

Columns A-C:	Tx value is a mapping from [x_min, x_max] to [-1,1]
Columns D-F:	Sx value is a rank value of the corresponding tx value. 1 is low, 2 is mid, 3 is high, 0 will not be included in integration
Column G:	Sample # value (1-27). 0 values will not be included in integration
Columns H-J:	Actual values of altitude (y), launch angle (theta), and muzzle velocity (vm) corresponding to the tx values from Columns A-C
Columns K-N:	Weights for numerical integration. Total weight is the product of the other three.
Column O:	Maximum height possible for the given muzzle velocity and launch angle
Columns P-Q:	The minimal and maximal altitudes where collision is possible
Columns R-S:	Calculations to determine expected relative velocities of shell and aircraft
Column T:	Duration (in seconds) that the shell spends in the collision altitudes
Column U:	The expected density of artillery shells in one unit of airspace
Column V:	The total relative volume covered by aircraft traveling at the relative speed for the duration of the vulnerable time.
Column W:	The collision intensity parameter
Column X:	Probability of one or more shells in a single aircraft’s path at any point in time during the vulnerable time
Column Y:	Weighted probability used for numerical integration
Columns Z-AA:	Flags if shell does not attain aircraft min (col Z) or max (col AA) altitude.

Bibliography

- Air, Land, Sea Application Center. *Kill Box: Multi-Service Tactics, Techniques, and Procedures for Kill Box Employment*. Joint Publication 3-09.24, June 2005.
- Alexander, B. "Aircraft Density and Midair Collision," *Proceedings of the IEEE*, 58 (3):377–381, 1970.
- Alfano, S. "Satellite Collision Probability Enhancements," *Journal of Guidance, Control, and Dynamics*, 0629(3):588–592, 2006.
- Alfriend, K. T., et al. "Probability of Collision Error Analysis," *Space Debris*, 1: 21–35, 1999.
- Baddeley, A., et al., editors. *Lecture Notes in Statistics*. Springer Science + Business Media Inc., New York, 2006.
- Ball, F. "A note on variation in birth processes," *Mathematical Scientist*, 20(1): 50–55, 1995.
- Ball, F. and Lynn, O. "Optimal vaccination schemes for epidemics among a population of households, with application to variola minor in Brazil," *Statistical Methods in Medical Research*, 15:481–497, 2006.
- Ball, F. and Donnelly, P. "Interparticle Correlation in Death Processes with Application to Variability in Compartmental Models," *Advances in Applied Probability*, 19(4):755–766, 1987.
- Bethea, D. and Herbranson, T. "Calculating the number of Aircraft volume boxes hit, within a certain airspace, by a ballistic following a simple trajectory,". Personal correspondence, 25 July, 2008.
- Bethea, D. and Herbranson, T. "Bullet Background Paper on Operations Research Fratricide Study,". Online Posting to Air Force Knowledge Now, Warfighter Applications COP, 11 2008.

- Bird/Wildlife Avian Strike Hazard (BASH) Team. "United States Avian Hazard Advisory System," 2008. Available online at: usahas.com (Accessed: 3/2/2009).
- Brix, A. and Chadoeuf, J. "Spatio-temporal modeling of weeds and shot-noise G Cox processes," *Biometrical Journal*, 44:83–99, 2002.
- Brown, T. C. and Donnelly, P. "On Conditional Intensities and on Interparticle Correlation in Non-Linear Death Processes," *Advances in Applied Probability*, 25: 255–260, 1993.
- Brush, S. G., editor. *Kinetic Theory, Vol. I: the Nature of Gases and Heat*. Pergamon Press, Ltd, Oxford, 1965.
- Burden, R. L. and Faires, J. D. *Numerical Analysis, 6th ed.* Thompson Brooks/Cole, Belmont, CA, 2005.
- Campbell, M. "Ball hits dove. 1-in-13-million odds. Dove not amused.," *The Globe and Mail*, F9, 31 March 2001.
- Carlton-Wippern, K. C. "Analysis of Satellite Collision Probabilities due to Trajectory and Uncertainties in the Position/Momentum Vectors," *Journal of Space Power*, 12(4):349–364, 1993.
- Carpenter, J. R. "Non-Parametric Collision Probability For Low-Velocity Encounters," *Advances in the Astronautical Sciences*, 127(1):227–242, 2007. Argues for Monte-Carlo simulation of satellite collisions.
- Chan, K. F. "Collision Probability Analyses for Earth Orbiting Satellites," *Advances in the Astronautical Sciences*, 96:1033–1048, 1997.
- Chan, K. "Short-term vs. Long-term Spacecraft Encounters," In *Proceedings of the AIAA/AAS Astrodynamics Specialist Conference and Exhibit*, Providence, RI, August 2004.
- Chapman, C. R. and Morrison, D. "Impacts on the Earth by Asteroids and Comets: Assessing the Hazard," *Nature*, 367:33–7, 1994.

- Chiang, Y.-J., et al. "Geometric Algorithms for Conflict Detection/Resolution in Air Traffic Management," In *Proceedings of the 36th Conference on Decision & Control*, San Diego, CA, December 1997.
- Clausius, R. *On the Mean Lengths of Paths Described by the Separate Molecules of Gaseous Bodies*, 135–147. In Brush (1965), 1858.
- Comas, C. and Mateu, J. "On soft and hard particle motions for stochastic marked point processes," *Journal of Statistical Computation and Simulation*, 77:1091–1121, 2007. doi: 10.1080/10629360600864217.
- Daly, M., editor. *Jane's Unmanned Aerial Vehicles and Targets, Issue 30*. Jane's Information Group, Inc., Alexandria, VA, 2008.
- DeAngelis, A. "Is It Really Worth Running in the Rain?," *European Journal of Physics*, 8(3):201–2, 1987.
- Faddy, M. J. "Non-linear stochastic compartmental models," *IMA Journal of Mathematics Applied in Medicine and Biology*, 2:287–297, 1985.
- Faddy, M. J. "On Variation in Birth Processes," *Advances in Applied Probability*, 22(2):480–483, 1990.
- Faddy, M. J. "On Variation in Poisson Processes," *Mathematical Scientist*, 19(1): 47–51, 1994.
- Faddy, M. J. "Markov process modelling and analysis of discrete data," *Applied Stochastic Models and Data Analysis*, 13:217–223, 1995.
- Faddy, M. J. "Extended Poisson Process Modelling and Analysis of Count Data," *Biometrical Journal*, 39(4):431–440, 1997.
- Faddy, M. J. "Markov death process modelling and analysis of binary data," *Statistics and Probability Letters*, 40:9–13, 1998.

- Faddy, M. J. and Smith, D. M. “Extended Poisson process modelling of dilution series data,” *Journal of the Royal Statistical Society, Series C: Applied Statistics*, 57:461–471, 2008.
- Faddy, M. J. and Smith, D. “Modeling the Dependence between the Number of Trials and the Success Probability in Binary Trials,” *Biometrics*, 61:1112–1114, 2005.
- Faddy, M., et al. “Likelihood-Based Modeling and Analysis of Possum Trapping Data,” *Journal of Agricultural, Biological, and Environmental Statistics*, 6:235–242, 2001.
- Fraser, D. A. S. “Generalized Hit Probabilities with a Gaussian Target,” *The Annals of Mathematical Statistics*, 22(2):248–255, 06 1951.
- Glen Shilland, M. U., February 2009. Personal Interview.
- Gross, D. and Harris, C. M. *Fundamentals of Queueing Theory, Third ed.* John Wiley & Sons, Inc., New York, 1998.
- “Guidance,” *Scottish Natural Heritage*, n. pag., 2000. Available online at: <http://www.snh.org.uk/pdfs/strategy/reneable/COLLIS.pdf> (Accessed: 09/29/2008).
- Hagenaars, T. J., et al. “Spatial heterogeneity and the persistence of infectious diseases,” *Journal of Theoretical Biology*, 229:349–259, 2004.
- Hensley, J. L. “A Fly Paper,” *Field Artillery Journal*, 12–16, May-June 1984. Available online at: http://sill-www.army.mil/FAMAG/1984/MAY_JUN_1984/MAY_JUN_1984_PAGES_12_16.pdf (Accessed: 3/2/2009).
- HQ Department of Army, United States Marine Corps. *Tactics, Techniques, and Procedures for Field Artillery Manual Cannon Gunnery (with Change 1)*. Field Manual 6-40 C1, December 1999.
- Inselmann, E. H. “The Generalized Zacks Model,”. Technical Report TP 12-77, 1977.

- Jenkin, A. B. and Gick, R. A. "Collision Risk Posed to the Global Positioning System by Disposal Orbit Instability," *Journal of Spacecraft and Rockets*, 39:532–538, 2002. doi: 10.2514/1.15398.
- Johnson, N. L., et al. "NASA's New Breakup Model of EVOLVE 4.0," *Advanced Space Research*, 28:1377–1384, 2001. doi: 10.1016/S0273-1177(01)00423-9.
- Johnson, R. E. *Introduction to Atomic and Molecular Collisions*. 1939.
- Joint Chiefs of Staff. *Joint Tactics, Techniques, and Procedures for Close Air Support (CAS)*. Joint Publication 3-09.3, September 2003.
- Kim, C. "The Effect of Sensor Performance on Save Minefield Transit," Master's thesis, Naval Postgraduate School, 2002. Available online at: <http://www.nps.edu/academics/gseas/usw/docs/NPSResearchNewsFebruary2003UnderseaWarfareResearchCenter.pdf> (Accessed: 3/2/2009).
- Loeb, L. B. *The Kinetic Theory of Gases*. McGraw-Hill Book Company, Inc., New York, 1934.
- Maxwell, J. C. *Illustrations of the Dynamical Theory of Gases*, 148–171. In Brush (1965), 1858.
- Microsoft® Corporation. *Microsoft® Office Excel® 2007 (12.0.6331.5000) SP1 MSO (12.0.6320.5000)* [computer software]. Microsoft® Corporation, Redmond, WA, 2006. (Microsoft product screenshot(s) reprinted with permission from Microsoft Corporation.).
- Møller, J. and Waagepetersen, R. P. *Statistical Inference and Simulation for Spatial Point Processes*. CRC Press LLC, Boca Raton, FL, 2004.
- Møller, J. and Waagepetersen, R. P. "Modern Statistics for Spatial Point Processes," *Scandinavian Journal of Statistics*, 34(4):643–684, 2006. Available online at: <http://www.math.aau.dk/~jm/NordstatPaper.pdf> (Accessed: 3/2/2009).

- Musselman, D. A. "Joint Fires Battlespace Deconfliction: Doctrinal Emphasis to Eliminate Airborne Fratricide," Master's thesis, Air Command and Staff College, Air University, 2008. Available online at: https://www.afresearch.org/skins/rims/q_mod_be0e99f3-fc56-4ccb-8dfe-670c0822a153/q_act_downloadpaper/q_obj_13439698-f81e-473d-a350-679e3eb59a8a/display.aspx?rs=enginespage (Accessed: 3/2/2009).
- Neuenswander, D. M. "Position Paper: Risk of fratricide with fixed wing aircraft and fires," 2008.
- Podlich, H. M., et al. "Likelihood Computations for Extended Poisson Process Models," *InterStat*, 1999. Available online at: <http://interstat.statjournals.net/YEAR/1999/articles/9909001.pdf> (Accessed: 2/12/2009). September #1.
- Podlich, H. M., et al. "Semi-parametric extended Poisson process models for count data," *Statistics and Computing*, 14:311–321, 2004.
- Pollack, A. F., et al. "Tomahawk Deconfliction: An Exercise in System Engineering," *John Hopkins Applied Physics Laboratory Technical Digest*, 18(1):79–89, 1997. Available online at: <http://www.jhuapl.edu/techdigest/td1801/pollack.pdf> (Accessed: 3/2/2009).
- Quigley, J. and Walls, L. "Nonparametric Bootstrapping of the Reliability Function for Multiple Copies of a Repairable Item Modeled by a Birth Process," *IEEE Transactions on Reliability*, 54(4), 2005.
- Reese, S. and Sondow, J. "Parabola," *MathWorld – A Wolfram Web Resource*, n. pag., 2009. Available online at: <http://mathworld.wolfram.com/UniversalParabolicConstant.html> (Accessed: 2/25/2009).
- Smith, K. A. "Joint Transformation of Aerial Interdiction by Enhancing Kill Box Operations," Master's thesis, Air Command and Staff College, Air University, 2006. Available online at: <https://research.maxwell.af.mil/papers/ay2006/acsc/Smith.pdf> (Accessed: 3/2/2009).

- Stoyan, D. “Hard Problems with Random Systems of Hard Particles,” 2003. Available online at: <http://isi.cbs.nl/iamamember/CD1/abstracts/papers/3108.pdf> (Accessed: 3/02/2009).
- Strike, Land Attack and Air Defense (SLAAD) Committee of the National Defense Industrial Association (NDIA). “Integration, Control and Deconfliction of Joint Fires Study, Vol 1,”. 2001. Available online at: http://www.ndia.org/Divisions/Divisions/StrikeLandAttackAndAirDefense/Documents/Content/ContentGroups/Divisions1/Strike,_Land_Attack_and_Air_Defense/PDFs15/concept_of_ops.pdf (Accessed: 2/25/2009).
- Toscas, P. J. and Faddy, M. J. “Fitting the Extended Poisson Process Model to Grouped Binary Data,” *Computational Statistics*, 20:595–609, 2005.
- Weisstein, E. W. “Hypersphere,” *MathWorld – A Wolfram Web Resource*, 2009. n. pag. (2/10/2009) <http://mathworld.wolfram.com/Hypersphere>.
- Wikipedia Contributors. “A-10 Thunderbolt II,” *Wikipedia, The Free Encyclopedia*, 2009a. n. pag. (2/25/2009) http://en.wikipedia.org/w/index.php?title=A-10_Thunderbolt_II&oldid=273332097.
- Wikipedia Contributors. “C-130 Hercules,” *Wikipedia, The Free Encyclopedia*, 2009b. n. pag. (2/25/2009) http://en.wikipedia.org/w/index.php?title=C-130_Hercules&oldid=270629986.
- Wikipedia Contributors. “C-17 Globemaster III,” *Wikipedia, The Free Encyclopedia*, 2009c. n. pag. (2/25/2009) http://en.wikipedia.org/w/index.php?title=C-17_Globemaster_III&oldid=273224299.
- Wikipedia Contributors. “F-15 Eagle,” *Wikipedia, The Free Encyclopedia*, n. pag., 2009d. Available online at: http://en.wikipedia.org/w/index.php?title=F-15_Eagle&oldid=273027584 (Accessed: 2/25/2009).

Wikipedia Contributors. "F-16 Fighting Falcon," *Wikipedia, The Free Encyclopedia*, n.pag., 2009e. Available online at: <http://en.wikipedia.org/w/index.php?title=F-16\Fighting\Falcon&oldid=273246493> (Accessed: 2/25/2009).

Wikipedia Contributors. "F-16 Raptor," *Wikipedia, The Free Encyclopedia*, n.pag., 2009f. Available online at: <http://en.wikipedia.org/w/index.php?title=F-22\Raptor&oldid=272969998> (Accessed: 2/25/2009).

REPORT DOCUMENTATION PAGE

Form Approved
OMB No. 0704-0188

The public reporting burden for this collection of information is estimated to average 1 hour per response, including the time for reviewing instructions, searching existing data sources, gathering and maintaining the data needed, and completing and reviewing the collection of information. Send comments regarding this burden estimate or any other aspect of this collection of information, including suggestions for reducing this burden to Department of Defense, Washington Headquarters Services, Directorate for Information Operations and Reports (0704-0188), 1215 Jefferson Davis Highway, Suite 1204, Arlington, VA 22202-4302. Respondents should be aware that notwithstanding any other provision of law, no person shall be subject to any penalty for failing to comply with a collection of information if it does not display a currently valid OMB control number. **PLEASE DO NOT RETURN YOUR FORM TO THE ABOVE ADDRESS.**

1. REPORT DATE (DD-MM-YYYY) 15-03-2009		2. REPORT TYPE Master's Thesis		3. DATES COVERED (From — To) Mar 2008 — Mar 2009		
4. TITLE AND SUBTITLE Probabilistic Estimation of Rare Random Collisions in 3-Space				5a. CONTRACT NUMBER		
				5b. GRANT NUMBER		
				5c. PROGRAM ELEMENT NUMBER		
6. AUTHOR(S) Holzmann, Timothy Capt, USAF				5d. PROJECT NUMBER		
				5e. TASK NUMBER		
				5f. WORK UNIT NUMBER		
7. PERFORMING ORGANIZATION NAME(S) AND ADDRESS(ES) Air Force Institute of Technology Graduate School of Engineering and Management (AFIT/EN) 2950 Hobson Way WPAFB OH 45433-7765				8. PERFORMING ORGANIZATION REPORT NUMBER AFIT/GOR/ENS/09-07		
9. SPONSORING / MONITORING AGENCY NAME(S) AND ADDRESS(ES) Lemay Center Bikini Atoll Rd, SM 30 Los Alamos, NM 87545				10. SPONSOR/MONITOR'S ACRONYM(S) AFDDEC		
				11. SPONSOR/MONITOR'S REPORT NUMBER(S)		
12. DISTRIBUTION / AVAILABILITY STATEMENT Approval for public release; distribution is unlimited.						
13. SUPPLEMENTARY NOTES						
14. ABSTRACT A study of risk assessment for artillery fire randomly colliding with fixed wing aircraft is presented. The research lends itself to a general study of collision models. Current models of object collisions fall under one of three categories: the historical model, the gas particle model, and the satellite model. These three vary in data requirements and mathematical representation of the impact event. The gas particle model is selected for its flexibility and robust estimation. However, current mathematical development in the literature does not include certain spatial and dynamic components necessary for a general encounter (collision) model. These are derived in this work. For the specific application at hand Quadratic formulas estimate the ballistic arc of artillery shells to provide instantaneous relative velocities. An extended Poisson spatial process is applied over the relative volume within a collision radius during the conflict time window to provide a probability of collision. Implementation of the model for military use has been achieved via an Excel spreadsheet providing scenario study capability in real time. Results for several scenarios are presented which have been validated by experts. These results support current policy of strict deconfliction.						
15. SUBJECT TERMS Stochastic model, Kinetic theory, Encounter, Collision, Extended Poisson process, Spatial point process						
16. SECURITY CLASSIFICATION OF:			17. LIMITATION OF ABSTRACT	18. NUMBER OF PAGES	19a. NAME OF RESPONSIBLE PERSON	
a. REPORT	b. ABSTRACT	c. THIS PAGE			Jeffery Cochran, Phd, (ENS)	
U	U	U	UU	92	19b. TELEPHONE NUMBER (include area code) (937) 785-3636; e-mail: jeffery.cochran@afit.edu	